



Tripolar configuration and pulse shape in cochlear implants reduce channel interactions in the temporal domain

Gunnar L Quass^{a,b,1,*}, Andrej Kral^{a,b,c}

^a Institute for AudioNeuroTechnology (VIANNA) & Department of Experimental Otolaryngology Clinics, Hannover Medical School, Hannover, Germany

^b Cluster of Excellence "Hearing4All" (EXC 2177), Germany

^c Australian Hearing Hub, School of Medicine and Health Sciences, Macquarie University, Sydney, Australia

ARTICLE INFO

Keywords:

Channel interactions
Spread of excitation
Duration coding
Polarity
Pseudomonophasic pulse
Monophasic pulse
Common ground
Bipolar

ABSTRACT

The present study investigates effects of current focusing and pulse shape on threshold, dynamic range, spread of excitation and channel interaction in the time domain using cochlear implant stimulation. The study was performed on 20 adult guinea pigs using a 6-channel animal cochlear implant, recording was performed in the auditory midbrain using a multielectrode array. After determining the best frequencies for individual recording contacts with acoustic stimulation, the ear was deafened and a cochlear implant was inserted into the cochlea. The position of the implant was controlled by x-ray. Stimulation with biphasic, pseudomonophasic and monophasic stimuli was performed with monopolar, monopolar with common ground, bipolar and tripolar configuration in two sets of experiments, allowing comparison of the effects of the different stimulation strategies on threshold, dynamic range, spread of excitation and channel interaction. Channel interaction was studied in the temporal domain, where two electrodes were activated with pulse trains and phase locking to these pulse trains in the midbrain was quantified. The results documented multifactorial influences on the response properties, with significant interaction between factors. Thresholds increased with increasing current focusing, but decreased with pseudomonophasic and monophasic pulse shapes. The results documented that current focusing, particularly tripolar configuration, effectively reduces channel interaction, but that also pseudomonophasic and monophasic stimulation and phase duration intensity coding reduce channel interactions.

1. Introduction

Cochlear implant (CI) stimulation typically employs symmetric, biphasic, charge-balanced electrical pulses in the monopolar configuration (Loizou, 1999; Zierhofer et al., 1995; Kral & Tillein, 2021). To increase the loudness of a CI stimulus, the current pulse amplitude is increased. While providing a louder percept, this unfortunately increases current spread and by that channel interactions (White et al., 1984; Kral et al., 1998; Bierer & Middlebrooks, 2004). Increased spread of excitation and spectral smearing thus ultimately decrease speech understanding (Başkent, 2006; Throckmorton & Collins, 2002).

Channel interactions occur when two electrodes stimulate overlapping populations of neurons. In the most extreme case, two electrodes excite the same population of neurons. Speech understanding with CI makes use of the spectral information conveyed by the electrode

location. Spread of excitation is the reason why speech understanding in quiet peaks at six to eight effective channels, despite many more electrodes available on the implant (Fishman et al., 1997; Friesen et al., 2001; Berg et al., 2022). To increase the yield and efficacy of the electrodes, and thus to add channels of information, efforts have been undertaken to reduce the spread of excitation. Notably, multipolar current focusing methods from bipolar-, tripolar- to phased-array-stimulation are capable of narrowing the electric field (Kral et al., 1998; Bierer, 2007; Bierer et al., 2010; Arenberg Bierer, 2010; van den Honert & Kelsall, 2007). However, they did not translate to enhanced speech understanding (Mens & Berenstein, 2005; Berenstein et al., 2008), likely due to the uneven distribution of surviving spiral ganglion cells (Nadol, 1990; Jahn & Arenberg, 2019). Multiple current sources on the stimulation device are further required for current focusing.

Another parameter that influences the current spread and thus the

* Corresponding author at: Institute for AudioNeuroTechnology (VIANNA) & Department of Experimental Otolaryngology Clinics, Hannover Medical School, Hannover, Germany.

E-mail address: gquass@med.umich.edu (G.L. Quass).

¹ Kresge Hearing Research Institute, University of Michigan, Ann Arbor, MI, USA.

<https://doi.org/10.1016/j.heares.2024.108953>

Received 1 November 2023; Received in revised form 8 January 2024; Accepted 11 January 2024

Available online 19 January 2024

0378-5955/© 2024 The Author(s). Published by Elsevier B.V. This is an open access article under the CC BY-NC-ND license (<http://creativecommons.org/licenses/by-nc-nd/4.0/>).

spread of excitation is the pulse shape, namely the relation of phase duration to -amplitude and the symmetry between phases of the pulses. Biphasic symmetric pulses are commonly used in CI due to safety reasons (balanced charge distribution). However, an increasing body of evidence suggests that anodic- and cathodic stimulation have different effects: While cathodic stimuli mostly excite spiral ganglion neurons at or near the soma, anodic stimuli activate the neurons at the central axon (experimental evidence: Miller et al., 1998; Shepherd & Javel, 1999; Konerding et al., 2022; modelling data: Kalkman et al., 2022). In clinical studies, anodic-leading stimulation was shown to require lower stimulation currents than cathodic-leading pulses at equal loudness (Jahn and Arenberg, 2019; Undurraga et al., 2013), and produce a broader spread of excitation at equal currents (Spitzer and Hughes, 2017). Strong phase effects have also been observed with facial nerve stimulation: pseudo-monophasic pulses with short anodic phase can prevent facial nerve stimulation (Gärtner et al., 2022; Konerding et al., 2023). Phase effects on auditory thresholds differ in different studies (Miller et al., 1998; Miller et al., 1999; Macherey & Cazals, 2016; Konerding et al., 2022).

There are, however, complex interaction effects between stimulus polarity and electrode distance to the modiolus, pulse shape, and neural degeneration (Heshmat et al., 2021). What is more, alternative ways to deliver the charge to the tissue, such as use of pseudomonophasic- or ramped pulses (Van Wieringen et al., 2005; Macherey et al., 2006; Navntoft et al., 2020; Quass et al., 2020), may strongly influence polarity effects. Therefore, we decided to analyze thresholds, dynamic range, spread of excitation, and channel interactions with respect to stimulation polarity, pulse shape, current level, and stimulation mode in their interdependence in a combined stimulation setup. We observed that channel interactions are affected not only by stimulation configuration, but modestly also by polarity and pulse shape.

2. Materials & methods

2.1. Animals & anesthesia

All procedures were approved by the local state authorities (Lower Saxony state office for consumer protection and food safety, LAVES approval No. 18/2844 and 20/3383) and were carried out in accordance with the guidelines of the European Community for the care and use of laboratory animals (EU VD 86/609/EEC) and the German Animal Welfare Act (TierSchG). A total of 20 young adult Dunkin Hartley guinea pigs (*Cavia porcellus*, Crl:HA) of either sex with a minimum weight of 325 g were used in this study (11 males, 9 females). Eight of these animals that were part of the multipolarity experiment have been previously reported on with respect to phase duration stimulation effects (Quass et al., 2020).

Before surgery, all animals received a pre-medication treatment of 0.5 g Bene-Bac® (Dechra Veterinary Products Deutschland GmbH, Aulendorf, GER) and 0.3 mg diazepam (Ratiopharm GmbH, Ulm, GER). Initial anesthesia was applied by subcutaneous injection of 50 mg/kg Ketamine (10 %, WDT, Garbsen, GER), 10 mg/kg Xylazine (Medistar, Ascheberg, GER), and 0.1 mg/kg Atropine (B.Braun, Melsungen, GER). Analgesia was provided by subcutaneous injection of 0.05 ml Carprofen (Rimadyl, Pfizer Deutschland GmbH, Berlin, GER). All animals received a subcutaneous infusion of Ringer's solution at 2 ml/h. During the experiment, the animals were placed on a heating pad controlled by a rectal probe set to 37.6°C, and were artificially ventilated through a tracheotomy. Anesthesia was maintained on a surgical level throughout the entire experiment by volatile application of isoflurane (0.5 – 1.7 %, Baxter, Unterschleißheim, GER), and controlled by adjusting the concentration of isoflurane, the breathing rate, and the tidal volume. The heart rate, end-tidal CO₂, and temperature were continuously monitored during the experiment and kept stable by adjusting the anesthesia.

2.2. Surgical procedure

The surgical procedures were carried out under surgical anesthesia, have been described in detail previously (Quass et al., 2020) and will be briefly reiterated here. Surgery was always performed on the ear that exhibited better ABR-thresholds to click stimuli, or the right ear if both ears were equally sensitive. After receiving the tracheotomy, animals were head-fixed to a stereotaxic frame using a head bar that was glued to the skull with dental cement. The cochlea was first made accessible by opening the bulla dorso-caudal to the ear. The skull was then opened in a circle of 7 mm diameter, centered on stereotaxic coordinates (Bregma + 1.25 cm AP, - 0.45 cm ML) over the left hemisphere, using a dental drill. To access the IC, a 2 × 16 channels standard electrode array (A32 100-500-177, NeuroNexus Technologies, Ann Arbor, MI, USA) was inserted 3 - 5 mm at an angle of 30° – 45° from the vertical plane. After acoustic measurements were completed, a cochleostomy was performed by carefully drilling an opening of 0.7 mm diameter into the scala tympani of the basal turn without removing the IC electrode array. The animal was then deafened by intracochlear application of 10% neomycin / NaCl solution for 15-30 minutes. The neomycin was washed out by slow intrascalar application of Ringer's solution, and ABR measurements were performed to confirm deafness of the animal (lack of ABR responses up to at least 120 dB SPL). The process was repeated if necessary. A 6-channel research CI (Oticon medical, Smørum, DEN) with a length of 7 mm and 1 mm pitch was then slowly inserted into the scala tympani, and a silver ball electrode was implanted between the bone and muscle in the scruff as a return electrode. All implanted parts were then affixed to the animal using a tissue adhesive (Histoacryl, B.Braun, Melsungen, GER) to prevent dislocation. Upon completion of the experiment, animals received a lethal intracardiac injection of pento-barbital (Release, WDT, Garbsen, GER). The brain and the implanted cochlea were extracted and fixed in 4 % PFA for subsequent analysis. An overview of the electrode placement and insertion technique is shown in Fig. 1A.

2.3. ABR recordings

Prior to the experiment and after deafening, auditory brainstem responses (ABR) to click stimuli were recorded from both ears using three transcutaneous silver wire electrodes placed on the top of the skull above the vertex, behind the bulla, and a ground electrode in the scruff. Condensation clicks of 50 μs duration were presented monaurally through a calibrated in-ear loudspeaker (DT 48, Beyer Dynamics, Heilbronn, GER) 100 times from 0 dB SPL peak equivalent to 80 dB SPL peak equivalent in steps of 5 dB. The signals were amplified (1000x) and filtered (0.5 kHz – 2 kHz) online, and low-pass filtered at 100 Hz offline.

2.4. Frequency mapping

Before pharmacological deafening, acoustic frequency tuning was recorded in order to localize the IC and to determine the spread of excitation of the electrical stimulation. Acoustic stimuli were generated at 1 MHz in AudiologyLab (Otoconsult, Frankfurt a.M., GER), and presented via a calibrated in-ear loudspeaker (DT 48). Mapping was performed over a range of 4 octaves spanning frequencies from 2 kHz to 32 kHz in steps of quarter octaves. Each 10 ms pure tone stimulus (2 ms cosine ramp) was presented 20 times at intensities from 0 dB SPL to 80 dB SPL in steps of 5 dB, and presentation was pseudo-randomized across frequencies and intensities. Responses are given as “spikes per stimulus” and represent all recorded suprathreshold events in a 25 ms post-stimulus analysis window (see “Recording & Data Analysis”).

2.5. Electrical stimulation

Electrical stimuli were generated in MATLAB (MathWorks, Natick, MA) at 100 kHz and presented via an optically isolated constant current

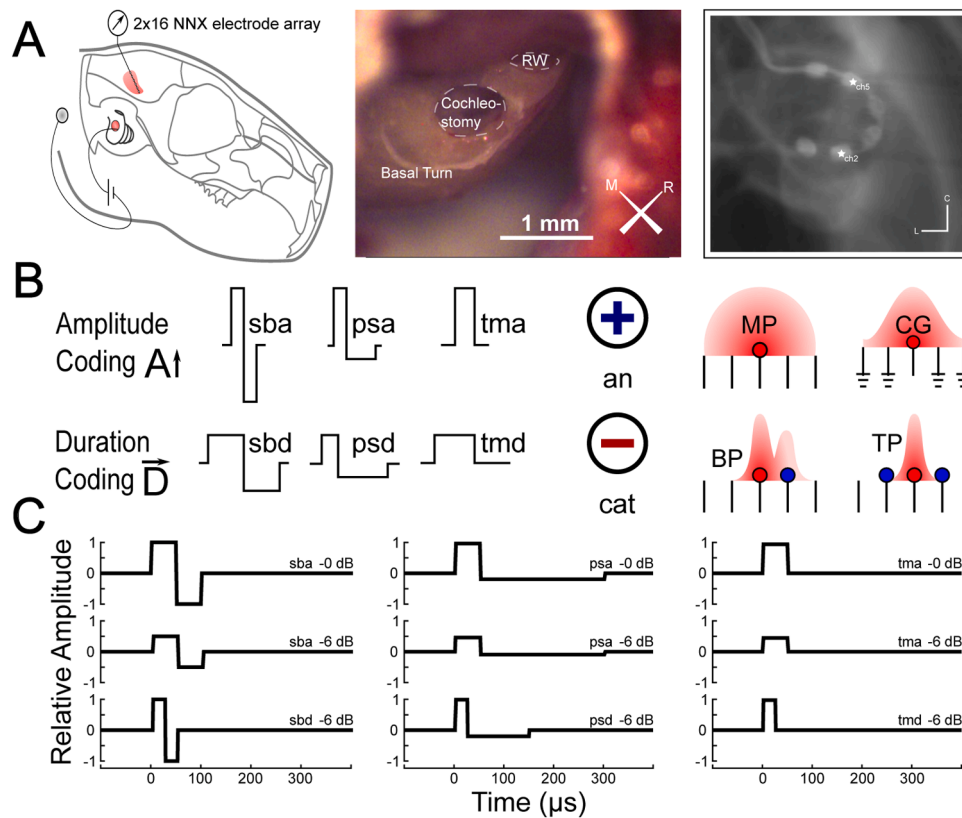


Fig. 1. Experimental approach. A – Left: schematic of the electrode placement. The recording electrode was inserted into the IC and oriented along the tonotopic gradient. The cochlear implant was advanced through a cochleostomy, and the extracochlear return electrode was placed in the scruff. Middle: photograph of the cochlear preparation. RW = round window. Right: CT micrograph of the inserted cochlear implant. ch2 = electrode 2 of the CI; ch5 = electrode 5 of the CI. B – Summary and legend of stimulus conditions. C – Comparison of stimulation waveforms at 0, -6, and 6 dB for standard biphasic- (sb, left), pseudomonophasic- (ps, middle), and true monophasic pulses (tm, right). For further abbreviations, see Table 1.

source (CS2, Otoconsult, Frankfurt a.M., GER) through the CI. Due to temporal constraints, we had to divide the parameter space into two experimental sets as follows (Table 1):

- (1) For the **common ground experiment**, stimuli were presented in all combinations of the following factors: “**Stimulus Shape**” (standard biphasic [sb], pseudomonophasic [ps], true monophasic [tm]), “**Coding Strategy**” (amplitude coding [-a], duration coding [-d]), “**Polarity**” (cathodic leading [CAT], anodic leading

[AN]), and “**Configuration**” (monopolar [MP], common ground/distributed all-polar [CG]).

- (2) For the **multipolarity experiment**, stimuli were always presented as cathodic-leading, and as a combination of “**Stimulus Type**” (standard biphasic with amplitude coding [sba], pseudomonophasic with amplitude coding [psa], pseudomonophasic with duration coding [psd]), and “**Configuration**” (monopolar [MP], bipolar [BP], tripolar [TP]). Electrical stimulus conditions are summarized in Fig. 1.

Table 1
Experimental setup and abbreviations used in the text.

Experimental Set	Factors	Parameter	Abbreviation
Common Ground Experiment	Stimulus Type	Standard Biphasic	[sb]
		Pseudomonophasic	[ps]
		True Monophasic	[tm]
	Coding Strategy	Amplitude Coding	[a]
		Duration Coding	[d]
	Polarity	Cathodic Leading	[CAT]
		Anodic Leading	[AN]
Configuration	Monopolar	[MP]	
	Common Ground/ Allpolar	[CG]	
Multipolarity Experiment	Stimulus Type	Standard Biphasic, Amplitude Coding	[sba]
		Pseudomonophasic, Amplitude Coding	[psa]
		Pseudomonophasic, Duration Coding	[psd]
	Configuration	Monopolar	[MP]
		Bipolar	[BP]
		Tripolar	[TP]

As an example of nomenclature, the name “CAT-MP-sba” describes a cathodic leading (CAT), monopolar (MP), standard biphasic waveform (sb), using amplitude coding for intensity (a). A detailed view of electrical stimuli is given in Fig. 1. All waveforms were rectangular, had fixed phase duration and phase amplitude ratios, and no interphase gaps. Biphasic pulses had 50 μs phase durations at 0 dB, and a phase duration and amplitude ratio of 1:1. Pseudomonophasic pulses had a first phase duration of 50 μs and a second phase duration of 250 μs at 0 dB, a phase duration ratio of 1:5, and a phase amplitude ratio of 5:1. Monophasic stimuli had a first phase duration of 50 μs and no second phase. Stimulus intensity was coded either by increasing the phase amplitudes (-a), with an increase of 6 dB corresponding to a doubling of the respective amplitudes, or by increasing the phase durations (-d), with an increase of 6 dB corresponding to a doubling of the respective durations. The respective other parameter was held constant. For duration coding, the amplitude was held constant at the lowest amplitude that elicited a response in the IC for the respective amp-coded pulse as determined online. At 0 dB, all phases thus hold the same charge between conditions. Current-amplitude-coded stimuli were used to determine the response thresholds, and were presented at intensities

from -50 dB (corresponding to a peak current of 31.62 μ A and a charge per phase of 1.58 nC) to -15 dB (corresponding to a peak current of 1.77 mA and a charge per phase of 88.91 nC) in steps of 1 dB. In rare cases where the threshold was reached very close to -15 dB, intensity was increased further, up to -10 dB (corresponding to a peak current of 3.16 mA and a charge per phase of 158 nC).

After single pulse mapping, 800 ms pulse trains composed of single pulses as described above were presented at 0 dB, and +6 dB relative to the respective thresholds. These pulse trains were used to quantify the channel interactions. To this end, a 19 Hz pulse train stimulus was first presented in an “isolated” condition at electrode 2 (apical). After that, a 37 Hz pulse train was presented at electrode 5 (basal) simultaneously with the 19 Hz pulse train on electrode 2 in a “simultaneous” condition. The parameters were always the same for both stimuli when presented simultaneously.

2.6. Recording & data analysis

All IC neural traces were recorded through a 2×16 Ir/IrOx electrode array with $177 \mu\text{m}^2$ contacts spaced 100 μm longitudinally, and 500 μm laterally (NNX A32 100-500-177, initial impedance ca. 100 k Ω). Signals were amplified (Neuralynx Cheetah 64-channel amplifier, 8000x, Neuralynx, Bozeman, MT), bandpass-filtered at 0.1 Hz – 9 kHz, digitized (NI-6259, National Instruments, Austin, TX) at a sampling rate of 20 kHz, and stored using AudiologyLab. A small silver ball electrode was placed epidurally directly posterior to Bregma to serve as a reference.

All signals were further processed using custom MATLAB routines. Electrical artefacts were removed through linear interpolation. All individual signals were digitally bandpass-filtered at 300 Hz – 3000 Hz to extract multiunit activity (MUA). Events were extracted as described previously (Quiroga et al., 2004), and while we did not perform any spike sorting, we call suprathreshold events “spikes”. In brief, a spike was detected when the rectified signal amplitude exceeded three times the median rectified signal amplitude divided by 0.6745. A detection limit of 4 spikes per ms was set to account for refractory periods and the fact that we recorded MUA. Spikes were then binned into 1 ms bins to obtain peri-stimulus time histograms, and the “spikes per stimulus” were counted within a 25 ms post-stimulus window.

The best frequency (BF) was defined as the frequency that elicited the most spikes over all presented intensities, thus taking both the response strength as well as the thresholds into account. The electrical threshold was defined as the lowest intensity that elicited a spiking response that exceeded the mean ongoing spiking activity in a randomly selected 25 ms pre-stimulus window by at least 3 standard deviations. The dynamic range was defined as the range from 10% – 90% of the maximal response strength for a four-parameter logistic equation (sigmoid function) fitted to the firing rate/intensity level function individual to every recording channel. Only recording channels that reached a sufficient fit ($R^2 > 0.8$) were further analyzed. For the threshold analysis, we show the lowest recorded threshold (“best channel threshold”) since the electrical thresholds along the recording array were highly variable (depending to tuning width). In the rare case of multiple contiguous channels with the same threshold values, we chose the median channel along the depth of the IC. In the rare case of double-peaked excitation profiles, we chose the channel with the higher elicited spike rate.

The spread of excitation was calculated as the width of the activity along the IC array in octaves at 1 dB above threshold. To this end, we used the BFs assigned to each recording channel, and created functional tuning curves, or “excitation profiles”, by applying response thresholding as described above.

For electrical pulse trains, the vector strength (VS) was calculated as described before (Goldberg and Brown, 1969). Briefly, the periodic impulse stimuli were treated as sinusoidal periodic stimuli with a period duration equal to the interpulse duration. The spike occurrence times were then mapped onto the interpulse periods, resulting in a “period”

histogram. The VS was then computed for the main phase angle, reflecting the probability that a spike in a given period falls in the most likely time bin, and statistical significance was determined by a Rayleigh-test ($\alpha = 0.95$). Only responses that had significant VS ($p < 0.05$) were further analyzed.

2.7. Statistics

All statistical tests were performed using standard or custom-written MATLAB routines, with the exception of the Rayleigh test, which was performed using the Circular Statistics Toolbox (Berens, 2009). Absolute values are given as median and median absolute deviation (MAD). Where differences were compared, results are presented as means \pm standard deviation. N-way ANOVA was used to analyze the results of the multipolarity- and the common ground experiments separately, since they were recorded as two different data sets. All boxplots display the median and interquartile range as the box, and the whiskers contain all data points that are within 1.5 interquartile range of the nearest box edge. All remaining data points are marked as outliers in the figures, but are included in the data analysis.

3. Results

First, acoustic receptive fields of neurons in the inferior colliculus were determined and the best frequency (BF) of each recording site was identified (Fig. 2). These data provided detailed information on the spatial excitation in the cochlea. After pharmacological destruction of hair cells to prevent electrophony (direct electrical stimulation of surviving hair cells, Sato et al., 2016), cochlear implantation was performed with the recording midbrain multielectrode array in place. Using electric stimulation, electric receptive fields (“excitation profiles”) were determined with single pulses. Using monopolar configuration, receptive fields covered the whole range of recording sites (Fig. 2B). BP and TP receptive fields were significantly narrower (Fig. 2C, D).

Compared to the current focusing with BP and TP stimulation, the focusing effect was present but much smaller in common ground mode (Fig. 3). Thresholds substantially increased in all multipolar and common ground measurements compared to MP.

3.1. Thresholds and dynamic range

Best thresholds, dynamic range, and spread of excitation were analyzed using single pulse measurements. A summary plot of the recorded thresholds is shown in Fig. 4A, B, and the corresponding ANOVA is given in Tables 2, 3. When analyzed over the full set of stimuli in the common ground experiment, the ANOVA revealed a significant main factor “Pulse Shape” (sb, ps and tm, n-way ANOVA, $F(2|153) = 24.41$, $p < 0.001$). Pooled over all other factors, pseudomonophasic pulses decreased mean thresholds by 1.3 ± 1.5 dB (Fig. 4C) compared to biphasic pulses, and the thresholds for monophasic pulses were lower than for biphasic pulses by 2.7 ± 2.2 dB (Fig. 4D). For CG stimulation only, thresholds decreased in the order sba – sbd – psa – psd – tma – tmd, suggesting that a progressive reduction of counterphase amplitude reduces thresholds in CG stimulation. This was further reflected in an interaction effect between “Pulse Shape” and “Configuration” ($F(2|153) = 3.58$, $p < 0.05$). Interestingly, “Polarity” did not systematically influence the thresholds ($F(1|153) = 3.27$, $p = 0.07$), except in a complex interaction effect with “Pulse Shape” and “Configuration” ($F(2|153) = 4.06$, $p < 0.05$). In contrast, “Configuration” was a significant factor for both sets (ANOVA, $F(1|153) = 218.38$, $p < 0.001$ for the MP/CG set, and $F(1|71) = 24.51$, $p < 0.001$ for the MP/BP/TP set), with MP stimulation generally yielding the lowest thresholds at a median of 31 dB (MAD 2.6). In comparison, the median thresholds of BP and TP stimulation were 21 (MAD 2.2) and 20 (MAD 6.3) dB, respectively. While CG stimulation fell in-between the mono- and multipolar cases, the median thresholds were still 7 dB higher than for MP (MAD 2).

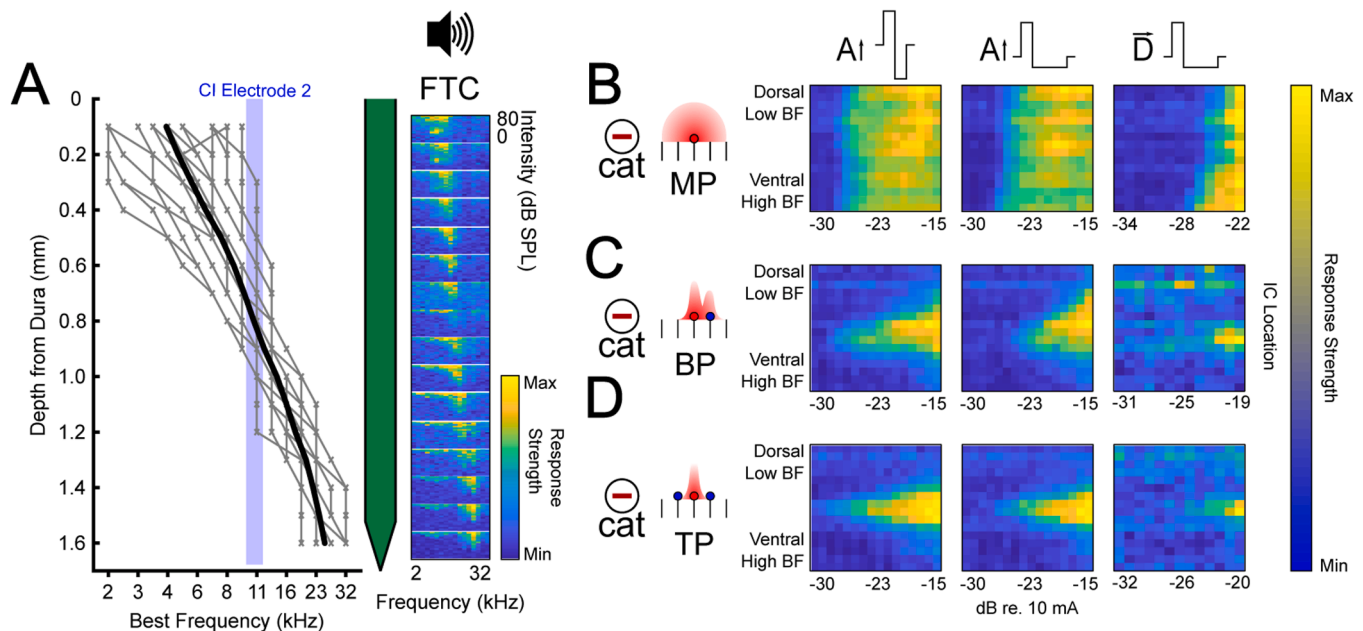


Fig. 2. Cochlear implant stimulation triggers responses in the IC. A – Summary of the recorded best frequencies (BFs) per electrode contact per animal (grey lines), and the average BF profile (black line). The blue shading indicates the approximate location of the mainly stimulated electrode 2 (approximately corresponding to 10–11 kHz). B – Normalized spiking responses (color coded) of IC electrodes plotted over stimulus intensity (x-axis) and recording electrode channel (y-axis) for cochlear electrode 2 monopolar stimulation during the multipolarity experiment (“Excitation Profiles”). Pulse shape and intensity coding strategy are shown above the plots. The approximate position of the stimulating electrode 2 was 11 kHz. FTC = frequency-threshold-characteristic; A = amplitude coding; D = duration coding; MP = monopolar configuration; cat = cathodic-leading. C – The same as B, but for bipolar stimulation. BP = bipolar configuration. D – The same as D, but for tripolar stimulation. TP = tripolar configuration. B-D are from the same animal.

For the **dynamic range** analysis, we used all channels that reached a sufficient fit. In the common ground experiment (Fig. 5, Table 4), “Coding” had the only significant main effect ($F(1|137) = 19.84$, $p < 0.001$). However, the effect was small – pooled over all conditions, duration coding led to a mean reduction of the median dynamic range by 0.21 ± 0.97 dB, explaining about 10% of the total variance. The highest median dynamic range was achieved using CAT-CG-tma pulses (4.45 dB), and the lowest was found for CAT-MP-psa pulses (2.9 dB, although not a statistically significant difference within its group). No significant differences were found between the MP and CG electrode configurations ($F(1|137) = 1.14$, $p = 0.29$, Fig. 5C). In contrast, the median dynamic range recorded for BP and TP stimulation was considerably higher than for MP stimulation ($F(2|55) = 16.36$, $p < 0.001$, 3.45 and 5.1 dB, respectively, Fig. 5D,E), with “Pulse Shape” not impacting the dynamic range significantly ($F(2|55) = 0.01$, $p = 0.99$, Table 5).

3.2. Spread of excitation

To assess the spread of excitation, tuning-curve bandwidths at 1 dB above the threshold were determined in octaves (Fig. 6A). We used 1 dB above threshold to avoid ceiling effects resulting from the very high spread of excitation for MP and CG stimulation that was reached at ~3 dB above threshold. While this is potentially a soft level perceptually, it is consistently equally above threshold without risking exceeding the dynamic range (saturation) in any setting used.

The median spread of excitation was 1.75 octaves for CAT-MP-sba stimulation, and there was no effect of “Polarity” (N-way ANOVA, $F(2|153) = 0.01$, $p = 0.94$, Fig. 6B, Table 6). Interestingly, the CG configuration did not significantly influence the spread of excitation compared to MP stimulation ($F(2|153) = 2.12$, $p = 0.12$). For BP and TP stimulation, we observed an extensive reduction of the spread of excitation ($F(2|71) = 17.7$, $p < 0.001$, Fig. 6C, Table 7). While “Pulse Shape” was a significant factor ($F(2|153) = 4.75$, $p = 0.01$), this was likely driven by the small spread of excitation achieved with anodic leading, true monophasic (AN-tm) stimulation. When pooling across all other

parameters, the median difference in spread of excitation between pseudomonophasic and biphasic pulses was 0 (MAD = 0.90, Fig. 6D), while the difference between true monophasic and biphasic pulses was 0.75 (MAD = 1.1, Fig. 6E). In MP stimulation, there was a large difference between the median spread elicited by CAT-MP-tm and the one elicited by AN-MP-tm stimulation (2.5 with MAD = 0.87 octaves and 0.5 with MAD = 0.7 octaves, respectively, Fig. 6F), where AN-MP-tm reduced the spread of excitation compared to sb, but CAT-MP-tm did not. In contrast, CG-tm pulses always decreased the spread of excitation, regardless of polarity. The mean spread of excitation pooled across pulse shapes for MP was 1.9 ± 1.2 octaves, for BP 1.1 ± 1.2 octaves, and for TP 0.4 ± 0.7 octaves, leading to a mean reduction by 0.5 octaves for BP (Fig. 6G) and 1.1 octaves for TP (Fig. 6H). For psa pulses, we found a reduction for TP (mean 0.1 ± 0.4 octaves), and an increase for BP (mean 2.2 ± 1.9 octaves). However, the ANOVA results in the multipolarity experiment revealed only a significant main effect of “Configuration”.

We assessed the spread of excitation growth over a range of 1 dB to 4 dB above threshold to verify if there are differences in the growth functions between the different stimuli (Fig. 7A-F). We found that overall, the slope of the spread of excitation growth functions was not different. An exception were anodic-leading true monophasic pulses (AN-tm, Fig. 7D,E), which showed a smaller spread of excitation at 1 dB above threshold compared to all other conditions. However, only monopolar, duration-coded stimuli (AN-MP-tmd) retained this advantage at higher intensities. Most growth functions shifted along the y-axis using different pulse shapes, in line with “Pulse Shape” being the only significant factor. “Intensity” also was a highly significant factor (N-way ANOVA, $F(3|707) = 19.61$, $p < 0.001$). However, there were no interaction effects.

3.3. Channel interactions

We quantified the channel interactions by measuring the degree of interference of a strong stimulus presented on electrode 5, to the response to a strong stimulus presented on electrode 2 (+6 dB). Since

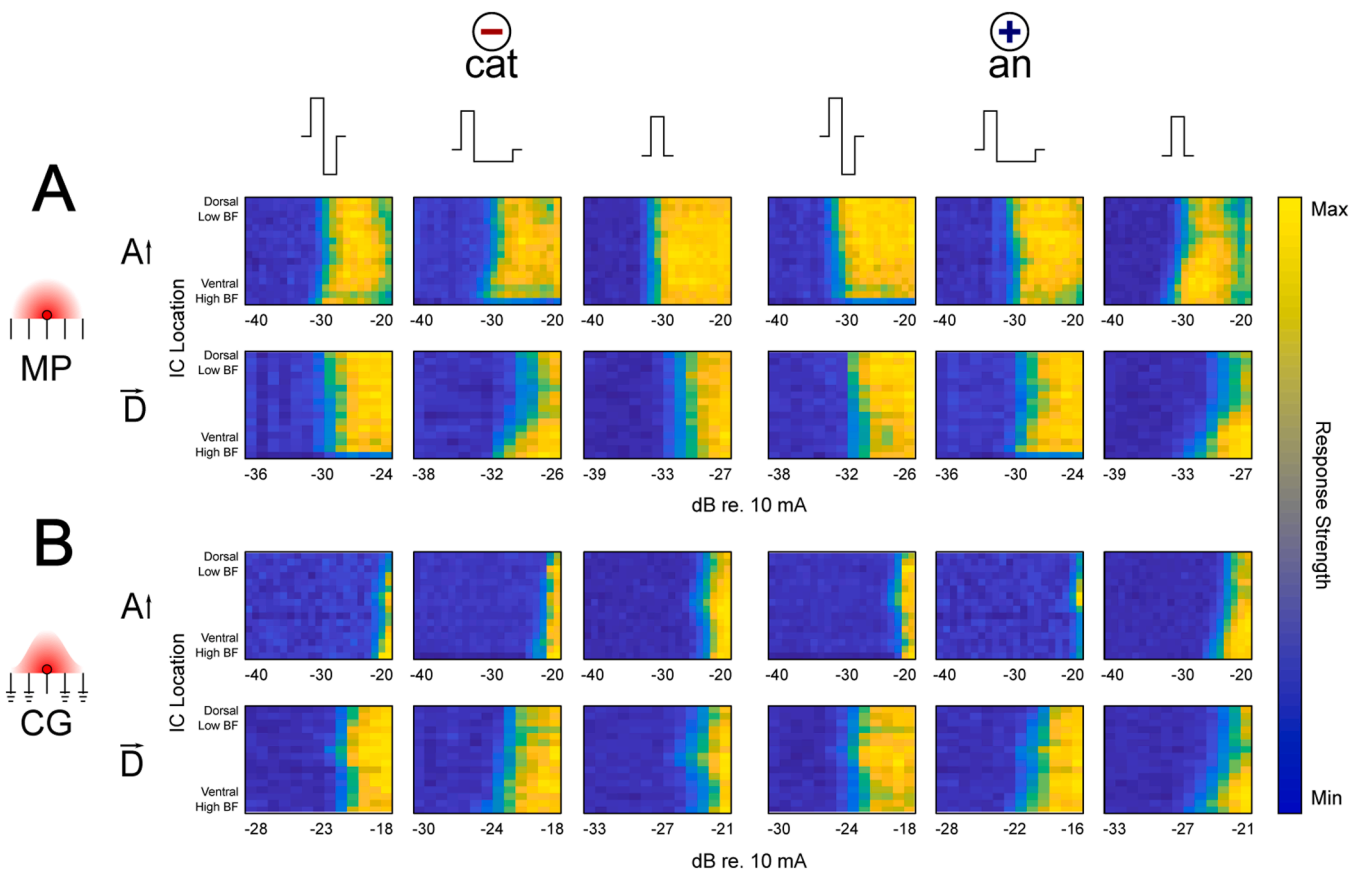


Fig. 3. Excitation profiles for monopolar and common ground stimulation in the same animal. A – Normalized spiking responses (color coded) of IC electrodes plotted over stimulus intensity (x-axis) and recording electrode channel (y-axis) for cochlear electrode 2 monopolar stimulation during the common ground experiment (“Excitation Profiles”). Pulse shapes are indicated above the plots, electrode configuration and intensity coding strategy to the left. B – The same for CG stimulation. The approximate position of the stimulating electrode 2 was 11 kHz. MP = monopolar configuration; CG = common ground configuration; A = current amplitude coding; D = pulse duration coding; cat = cathodic leading (cathodic pseudomonophasic or monophasic) stimulation; an = anodic leading (cathodic pseudomonophasic or monophasic) stimulation.

different pulse repetition rates were used at electrodes 2 and 5, phase locking to each pulse train can be quantified independently using vector strength (Fig. 8A; example poststimulus time histogram shown in Fig. 8B). This was first done in the isolated condition where only a single pulse train was presented. When subsequently presenting both pulse trains simultaneously, the vector strength can be determined again and related to the isolated condition, where only one electrode was active. This allows quantifying channel interactions by calculating the ratio of these vector strengths (see methods).

At the high intensities used here, the spread of excitation is likely high, since this stimulation exceeds the dynamic range (see Fig. 5), such that a high degree of spatially overlapping activation can be expected. The resulting measure is thus related to spread of excitation used above, however, with pronounced differences: first, our spread of excitation measure is a near-threshold measure, whereas channel interaction is a measure that captures the interactions at high current levels (here 6 dB above threshold). The spread of excitation is further reported exclusively for the activation of the apical electrode 2, while channel interactions include multi-channel, (closely) successive activations of electrodes 2 and 5. VS is a measure related to temporal processing of competing stimuli, whereas the spread of excitation reflects the spatial spread of an isolated stimulus. Finally, in addition to the peripheral spread of excitation, channel interaction as defined here includes central auditory neuronal interactions present on the level of the IC. This computational interaction more faithfully reflects a psychophysical channel interaction than the recording of separate spatial tuning curves, as it takes inhibitory and refractory effects into account, akin to forward

masking paradigms. Thus, channel interaction as quantified here is complementary to the spread of excitation measure used above. In other words, while a very low spread of excitation very likely directly results in a very high VS ratio (i.e., low channel interaction), a high spread of excitation does not need to result in a low VS ratio due to the reasons outlined above. Furthermore, the high suprathreshold intensity used for the VS ratio measurement (threshold +6 dB) would almost certainly result in much higher spread of excitation values, likely activating the entire cochlea in many cases.

VS ratio values above one correspond to an increase in phase locking to the original pulse train in the simultaneous conditions compared to the isolated condition, while values below one correspond to a decrease in phase locking. While both document an interference of the two pulse trains, the usual interaction was a decrease in phase locking. Values above 1 were only observed in cases when the phase locking to the first pulse train was rather weak and phase locking to the second pulse train was rather strong, usually leading to outliers in the datasets. Values equal to 1 reflect no interaction at all.

For CAT-MP-sba stimulation, we found a mean VS ratio of 0.24 ± 0.1 , while the mean VS ratio for CAT-BP-sba was 0.35 ± 0.22 . On average, the VS ratio for TP stimulation was very close to 1 (1.2 ± 0.45), meaning that there was only limited interaction and thus a much better channel separation. This tripolar result mirrors the low spread of excitation resulting in no or almost no overlapping activation in the IC. We did find a reduction of channel interactions by 7.6% for BP stimulation across all pulse shapes compared to MP, and a median enhancement for CAT-MP-psd compared to CAT-MP-sba by 1.7% (standard deviation

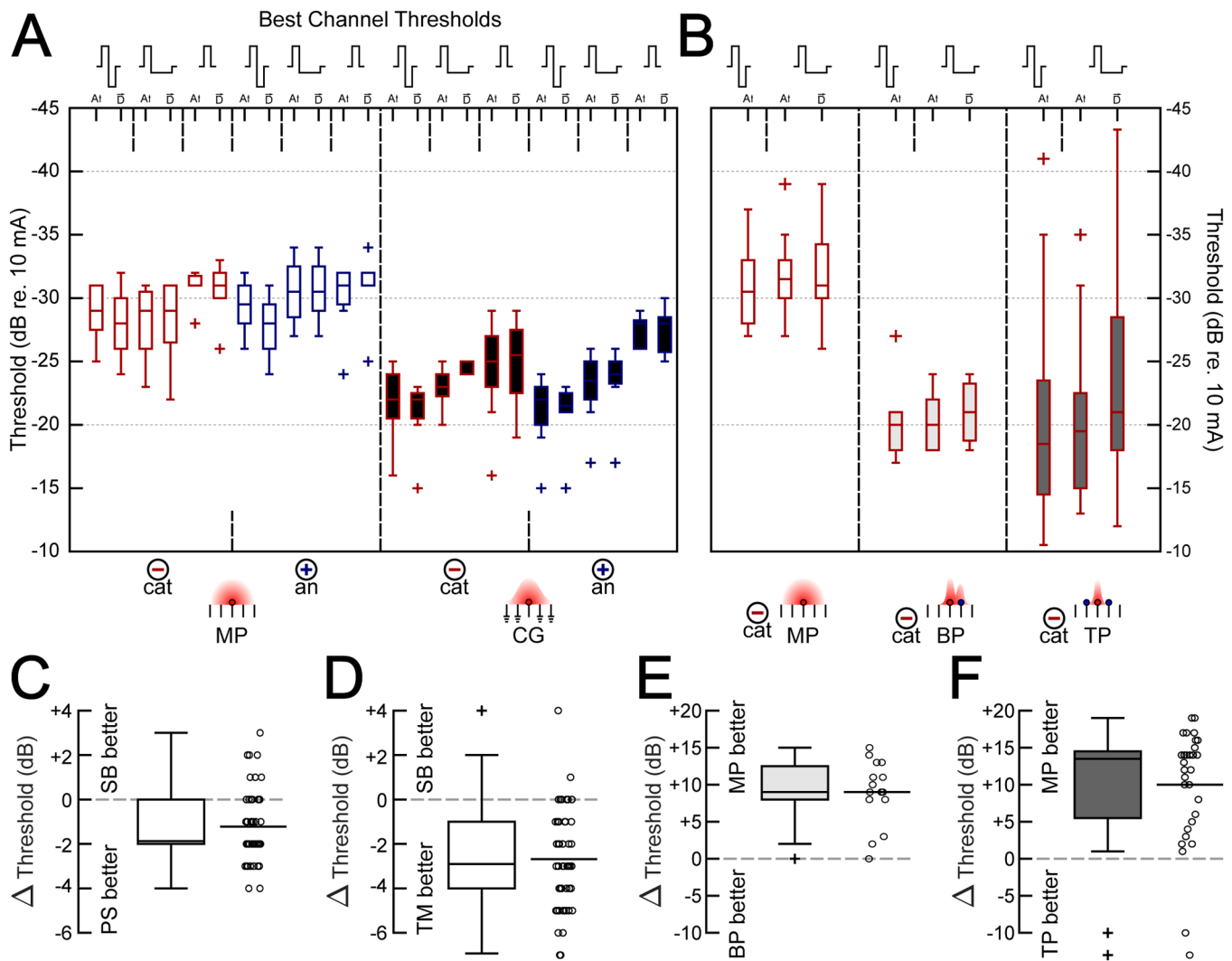


Fig. 4. Lowest thresholds per 16-channel recording for single pulses presented on electrode 2 on the CI for any given combination of stimulus properties. A – Common ground experiment. Pulse Shape and Coding Strategy are indicated above the boxes. Polarity is indicated by outline color (cat = red, an = blue). Electrode configuration is indicated by fill color (MP = white, CG = black). ANOVA revealed a significant effect of Pulse Shape and Configuration, with an interaction of Pulse Shape and Configuration and Pulse Shape, Polarity and Configuration. For details, see Table 2. B – The same as in A, but for the Multipolarity experiment. There is a significant effect of Configuration. For statistics see Table 3. C – Threshold distributions for all conditions pooled and compared between pseudomonophasic and biphasic pulse shapes. Scatter plot shows raw data and mean. D – Same as in C, but for true monophasic and biphasic pulse shapes. E – Same as C, but pooled and compared between bipolar configuration and monopolar configuration. F – Same as in E, but for tripolar and monopolar.

3.8%), as we have previously reported (Quass et al., 2020). While the ANOVA shows a significant main effect of “Stimulus Type”, this only accounts for 0.5% of the variance. The major contribution was made by “Configuration”, explaining 69% of the total variance.

In contrast, “Configuration” was the only factor that was not significant in the common ground experiment, meaning that CG did not show current focusing properties similar to those of BP and TP. Instead, we found that “Pulse Shape” was the strongest predictor for the VS ratio, accounting for about 11.6% of the variance in the common ground experiment. Generally, the negative channel interaction effects were reduced in the same order that was found for the thresholds: sba – sbd – psa – psd – tma – tmd, with the effect getting stronger from psd onward. Interestingly, this order was found for CAT stimuli only. For AN stimulation, the picture was less clear – the median VS ratio was increased only until psd, then reduced again for tma, and strongly increased for tmd for MP stimulation only. Potentially, more central stimulation with anodic stimulation (Konerding et al., 2022) favors channel interaction, which is mitigated by duration coding.

Within pulse shapes, duration coding was always superior to

amplitude coding (mean enhancement $9.63 \pm 15.6\%$). The same strict difference was not found for polarity, but there was an advantage of AN stimuli over CAT stimuli (mean enhancement $3.3 \pm 20.1\%$). One interesting observation are the large VS ratio values obtained for true monophasic stimulation with anodic polarity. This was likely the consequence of the small spread of excitation in this configuration (Fig. 6), yielding a similar effect as in tripolar configuration: adding the second train increases the VS due to the spillover effect in the first pulses and this is sufficient to substantially increase the ratio due to an increase of the originally very low VS in the isolated condition.

While there was no significant difference between MP and CG, there were significant interactions with all three other factors “Pulse Shape”, “Intensity Coding”, and “Polarity”. Specifically, the higher VS ratio achieved with pseudomonophasic pulses was greater using CG stimulation. The mean enhancement for MP was $7.2 \pm 12.1\%$, while the mean enhancement for CG was almost twice as great at $13.1 \pm 11\%$. Surprisingly, this relationship was not found for true monophasic stimuli when paired with duration coding, which lead to a $21.5 \pm 50\%$ improvement in MP stimulation, but only an $18.9 \pm 27\%$ enhancement

Table 2

N-way ANOVA results for the threshold measurements of the common ground experiment.

Factor	SSQ	dF	Mean SQ	F	p
Pulse Shape	342.89	2	171.44	24.41	<0.001***
Intensity Coding	0.03	1	0.03	0	0.95
Polarity	22.96	1	22.96	3.27	0.07
Configuration	1533.65	1	1533.65	218.38	<0.001***
Pulse Shape * Intensity Coding	15.92	2	7.96	1.13	0.32
Pulse Shape * Polarity	15.95	2	7.98	1.14	0.32
Pulse Shape * Configuration	50.35	2	25.17	3.58	0.03*
Coding * Polarity	0.05	1	0.05	0.01	0.94
Coding * Configuration	2.83	1	2.83	0.4	0.53
Polarity * Configuration	0.14	1	0.14	0.02	0.89
Pulse Shape * Intensity Coding * Polarity	1.03	2	0.52	0.07	0.93
Pulse Shape * Intensity Coding * Configuration	1.53	2	0.77	0.11	0.90
Pulse Shape * Polarity * Configuration	57.04	2	28.52	4.06	0.02*
Intensity Coding * Polarity * Configuration	0.41	1	0.41	0.06	0.81
Pulse Shape * Intensity Coding * Polarity * Configuration	4.59	2	2.3	0.33	0.72
Error	1074.5	153	7.02		
Total	3227.74	176			

Table 3

N-way ANOVA results for the Threshold measurements of the multipolarity experiment.

Factor	SSQ	dF	Mean SQ	F	p
Stimulus Type	27.01	2	13.505	0.35	0.71
Configuration	1898.79	2	949.939	24.51	<0.001***
Stimulus Type * Configuration	34.1	4	8.526	0.22	0.93
Error	2750.46	71	38.739		
Total	4869.19	79			

using CG stimulation.

Our distilled results are schematically summarized in Fig. 9.

4. Discussion

The strength of the present study lies in its complex cover of the stimulation parameter space using different stimulation configurations in only two experimental settings, including monophasic, pseudomonophasic, and biphasic stimuli, cathodic and anodic polarity, current-amplitude and pulse duration coding of stimulus intensity, and monopolar, bipolar, tripolar, and common ground electrode configurations. To the best of our knowledge, this is the first time these different settings were directly compared. While the recording was performed in the auditory midbrain as opposed to the auditory nerve, the midbrain is an obligatory nucleus of the auditory pathway that allows reliably assessing the excitation at the level of the cochlea using acoustic mapping of receptive fields.

The present study confirmed that current focusing strategies are effective in reducing the current spread, with the consequence of smaller spread of excitation and reduced channel interaction, but at the cost of higher stimulation thresholds. Tripolar configuration was most effective and showed nearly no channel interaction in the present study. Grounding of non-used contacts (common ground configuration as used in this study) was, however, not particularly effective in reducing the

current spread by itself, but retained the disadvantage of increasing the stimulation thresholds. Intensity coding using pulse duration provided some, albeit moderate, reduction in channel interactions as previously indicated (Quass et al., 2020), but was not effective in reducing the spread of excitation. The present experiments further documented an increase in dynamic range of electric stimulation with current focusing, most prominent in tripolar stimulation. Monophasic and pseudomonophasic pulse stimulation led to lower thresholds and less channel interactions than biphasic pulses.

Statistical analysis revealed a number of interactions between the tested stimulus parameters. In the given example of channel interactions, pulse shape, configuration (monopolar and common ground) and polarity significantly interacted. This suggests that when channel interactions are investigated, it is not sufficient to study these factors in isolation.

4.1. Current focusing

The present study demonstrates several beneficial effects of current focusing: not only does it reduce the spread of excitation in the cochlea, it also increases the dynamic range of the stimulation, and allows to provide better temporal information by reduced interaction between different channels. These benefits come at the cost of higher thresholds and the need for more energy in stimulation.

Both in previous animal experiments and in human studies, tripolar stimulation showed exquisite spatial focusing of stimulation (Kral et al., 1998; Bierer & Middlebrooks, 2004; Bonham & Litvak, 2008; Landsberger & Srinivasan, 2009). Phased array stimulation (van den Honert & Kelsall, 2007) showed a similar benefit, but did not provide a significant advantage compared to tripolar stimulation (George et al., 2015a; George et al., 2015b). Clinically, however, current focusing using tripolar stimulation did not translate to better speech reception (Mens & Berenstein, 2005; Berenstein et al., 2008). This is most likely related to a varying population of surviving spiral ganglion cells along the cochlear partition, leading to less robust information transfer in focused conditions – indeed, tripolar stimulation has been used as a tool to assess the variation of the spiral ganglion population along the cochlea (Arenberg Bierer, 2010).

Subjects stimulated with tripolar configuration further reported a decreased loudness of the stimulation (Mens & Berenstein, 2005; Berenstein et al., 2008), similar to radial stimulation, which also provides reduced thresholds and less current spread due to the direction of the electric current (Battmer et al., 1999). Low loudness is likely a direct consequence of the small spread of excitation, leading to limited integration of the excitation along the cochlear partition. Leveling this inherent drawback, however, complicates the clinical design of the speech processor, as this effect is not homogeneous along the cochlea and requires a custom setting for each channel individually (Arenberg Bierer, 2010). Partial tripolar strategies employing different amounts of return currents presented on the adjacent electrodes (σ -values, Kral et al., 1998, Mens and Berenstein, 2005; Berenstein et al., 2008) might be able to adjust the stimulation to the desired loudness level. However, as loudness growth functions are non-linear (Litvak et al., 2007), adapting the intensity in tripolar stimulation to a common loudness level likely further requires non-linear compression algorithms, which have so far shown only limited benefit for speech understanding (De Jong et al., 2019a, 2019b).

With respect to common ground stimulation, the present outcomes provide only limited support for this configuration. Similar or lower efficiency of common ground compared to bipolar stimulation in reducing the spread of excitation has been reported previously, as has the increase in threshold (Pfungst et al., 1997; Busby et al., 1994). Here, the threshold increase was larger than in previous studies, which likely had methodological reasons: in the present experiments the unused electrodes were connected to the stimulation ground, and thus drained the charge introduced in the cochlea by the active electrodes to 0 mV. In

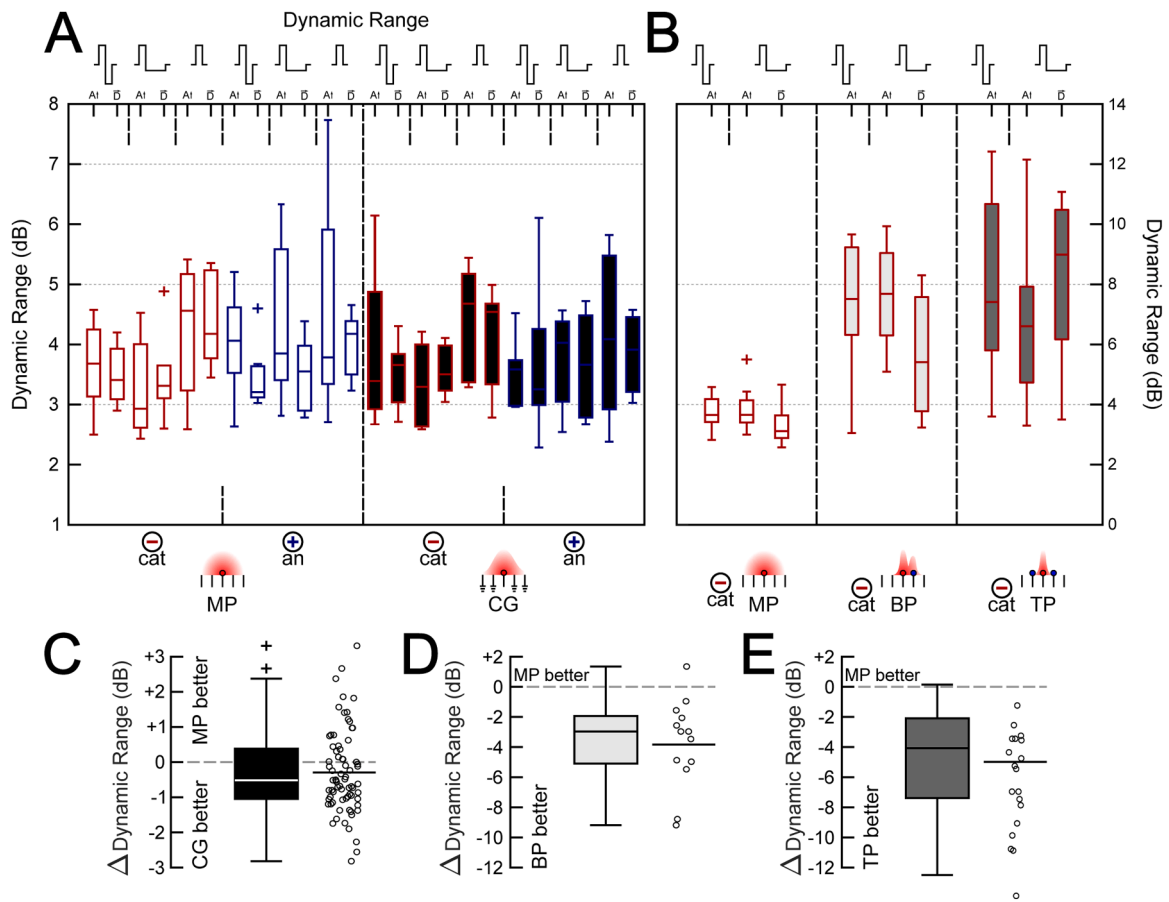


Fig. 5. Dynamic range distributions for single pulses presented on electrode 2 on the CI for any given combination of stimulus properties. A) Common ground experiment. ANOVA revealed a significant effect of coding. B) Multipolarity experiment. ANOVA revealed a significant effect of configuration. C – The difference in dynamic range between MP and CG pooled across other stimulation parameters. D – The same as C, but for BP and MP. E – The same as E, but for TP and MP.

Table 4

N-way ANOVA results for the dynamic range measurements of the common ground experiment.

Factor	SSQ	dF	Mean SQ	F	p
Pulse Shape	0.422	2	0.211	0.28	0.75
Intensity Coding	14.784	1	14.784	19.84	<0.001***
Polarity	1.471	1	1.471	1.97	0.16
Configuration	0.85	1	0.85	1.14	0.29
Pulse Shape * Intensity Coding	0.152	2	0.076	0.1	0.90
Pulse Shape * Polarity	2.141	2	1.071	1.44	0.24
Pulse Shape * Configuration	4.165	2	2.082	2.79	0.07
Coding * Polarity	0.008	1	0.008	0.01	0.92
Coding * Configuration	0.11	1	0.11	0.15	0.70
Polarity * Configuration	2.102	1	2.102	2.82	0.1
Pulse Shape * Intensity Coding * Polarity	1.719	2	0.859	1.15	0.32
Pulse Shape * Intensity Coding * Configuration	0.865	2	0.433	0.58	0.56
Pulse Shape * Polarity * Configuration	4.55	2	2.275	3.05	0.05
Intensity Coding * Polarity * Configuration	1.055	1	1.055	1.42	0.24
Pulse Shape * Intensity Coding * Polarity * Configuration	2.901	2	1.45	1.95	0.15
Error	102.072	137	0.7451		
Total	145.833	160			

Table 5

N-way ANOVA results for the dynamic range measurements of the multipolarity experiment.

Factor	SSQ	dF	Mean SQ	F	p
Stimulus Type	0.218	2	0.109	0.01	0.99
Configuration	271.946	2	135.973	16.36	<0.001***
Stimulus Type * Configuration	15.515	4	3.879	0.47	0.76
Error	457.033	55	8.31		
Total	756.732	63			

the clinical application there is no absolute ground available, and short-circuiting the unused electrodes to e.g. the implant body (“all-polar configuration”) only forces the same electrical potential at all electrodes. Therefore, the increase in thresholds observed in the present experiments might exceed the one observed in the clinical condition.

4.2. Coding loudness by phase duration

For single pulses, perceived loudness is a function of charge integrated over time (Parkins & Colombo, 1987; Pflugst et al., 1991; Chatterjee et al., 2000). Consequently, loudness can be coded by phase duration of the pulse, as opposed to amplitude. This duration coding has the additional advantage of influencing the current spread to a lesser degree compared to amplitude coding (Quass et al., 2020). Coding of loudness by phase duration as opposed to current amplitude was indeed robustly effective in reducing the channel interaction in the present study, albeit to a limited extent. This suggests that increasing the pulse

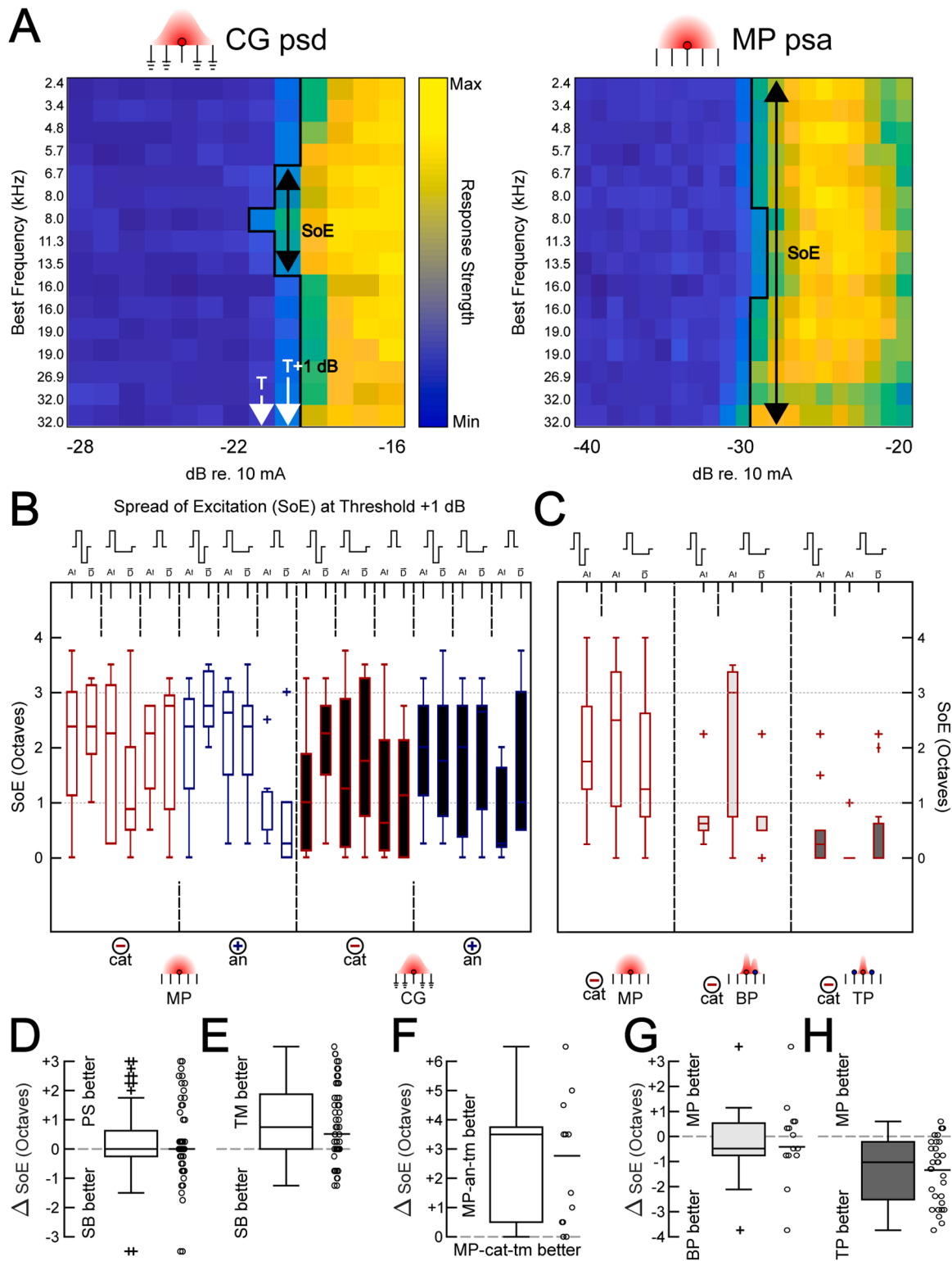


Fig. 6. Spread of Excitation as measured by tuning curve bandwidth in octaves. **A** – Example of the spread of excitation measurement for monopolar and common ground configurations. The plots are the normalized spike responses per channel and intensity (“Excitation Profiles”) also depicted in Fig. 3. One square in the y-direction equals one recording channel, with the recorded BF listed on the axis. One square in the x-direction equals 1 dB stimulus strength. The black line indicates the threshold border (white arrow on the x-axis labeled “T”) determined by the response thresholding. The spread of excitation was defined as the width of the black arrow (labeled “SoE”) at column T+1 (white arrow on the x-axis labeled “T+1 dB”) in octaves. In this case, the spread of excitation was 6.7 - 13.5 kHz ~ 1 octave for the common ground configuration, and 2.4 - 32.0 kHz ~ 4 octaves for the monopolar configuration. **B** – Spread of excitation for single pulses presented on electrodes 2 and 5 on the CI for any given combination of stimulus properties in the common ground experiment. Plot legend and layout are the same as in Figs. 4 and 5. ANOVA revealed a significant effect of Pulse Shape. For statistics, see Table 6. **C** – The same as in B, but for the multipolarity experiment. ANOVA revealed a significant effect of Configuration. For statistics, see Table 7. **D** – The difference in spread of excitation between pseudomonophasic and biphasic pulses pooled across all other stimulation parameters. **E** – The same as in D, but for true monophasic and biphasic. **F** – The difference in spread of excitation only for comparison of cathodic versus anodic MP true monophasic stimuli. **G** – The same as in D, but for BP and MP. **H** – The same as in D, but for TP and MP.

Table 6

N-way ANOVA results for the Spread of Excitation measurements of the common ground experiment.

Factor	SSQ	dF	Mean SQ	F	p
Pulse Shape	13.6	2	6.8	4.75	0.01
Intensity Coding	1.513	1	1.513	1.06	0.3
Polarity	0.008	1	0.008	0.01	0.94
Configuration	3.5	1	3.5	2.44	0.12
Pulse Shape * Intensity Coding	1.2	2	0.599	0.42	0.66
Pulse Shape * Polarity	6.072	2	3.036	2.12	0.12
Pulse Shape * Configuration	1.248	2	0.624	0.44	0.65
Coding * Polarity	0.032	1	0.032	0.02	0.88
Coding * Configuration	1.738	1	1.738	1.12	0.27
Polarity * Configuration	1.425	1	1.425	1	0.32
Pulse Shape * Intensity Coding * Polarity	1.298	2	0.649	0.45	0.64
Pulse Shape * Intensity Coding * Configuration	0.746	2	0.373	0.26	0.771
Pulse Shape * Polarity * Configuration	4.97	2	2.485	1.74	0.18
Intensity Coding * Polarity * Configuration	0.074	1	0.074	0.05	0.82
Pulse Shape * Intensity Coding * Polarity * Configuration	2.355	2	1.178	0.82	0.44
Error	219.005	153	1.4314		
Total	258.895	176			

Table 7

N-way ANOVA results for the Spread of Excitation measurements of the multipolarity experiment.

Factor	SSQ	dF	Mean SQ	F	p
Stimulus Type	2.559	2	1.28	1.21	0.3
Configuration	37.307	2	18.654	17.7	<0.001***
Stimulus Type * Configuration	5.319	4	1.33	1.26	0.29
Error	74.826	71	1.054		
Total	116.743	79			

duration leads to excess charge in the cochlea that may ultimately have a similar consequence as increasing the pulse amplitude. Furthermore, due to the leakiness of the neuronal membrane, the pulse duration also becomes less effective in injecting the charge into the neurons (Parkins & Colombo, 1987; Moon et al., 1993, for general review see Kral et al., 2021). In monophasic stimulation specifically, more effective intensity coding by phase duration was observed, very likely due to the excess charge at the double layer of the electrode that is typically eliminated by the opposite stimulation phase in biphasic stimulation. This result is worth follow-up studies.

4.3. Polarity effects

Cathodic (or cathodic-leading) stimulation results in lower thresholds than anodic stimulation in well-controlled animal studies (Miller et al., 1998; Hartmann et al., 1984), however, this also depended on the exact species and stimulation strategy: Cats had lower thresholds with cathodic stimulation, but guinea pigs with anodic stimulation (Miller et al., 1998). In a recent study, no differences were observed in guinea pigs (Konerding et al., 2022), and no difference for guinea pigs was observed in the present study either. Statistically, the present approach with several different pulse shapes should provide more robust information on the effect of polarity compared to previous experiments. The distance to the stimulating site was identified as a key confounding factor influencing the thresholds, potentially stronger than polarity (Miller et al., 1999), however, we did not control for this aside from always stimulating electrode 2. In human studies, lower most comfortable levels were reported for anodic stimulation using pulse trains

Table 8

N-way ANOVA results for the vector strength ratio Channel Interaction measurements of the common ground experiment.

Factor	SSQ	dF	Mean SQ	F	p
Pulse Shape	49.332	2	24.666	159.41	<0.001***
Intensity Coding	9.922	1	9.922	64.12	<0.001***
Polarity	1.752	1	1.752	11.32	<0.001***
Configuration	0.166	1	0.166	1.07	0.3
Pulse Shape * Intensity Coding	10.696	2	5.348	34.56	<0.001***
Coding					
Pulse Shape * Polarity	5.378	2	2.689	17.38	<0.001***
Pulse Shape * Configuration	5.334	2	2.667	17.24	<0.001***
Configuration					
Coding * Polarity	0.178	1	0.178	1.15	0.28
Coding * Configuration	1.263	1	1.263	8.16	<0.01**
Polarity *	1.341	1	1.341	8.67	0.03*
Configuration					
Pulse Shape * Intensity Coding * Polarity	2.42	2	1.21	7.82	<0.001***
Coding * Polarity					
Pulse Shape * Intensity Coding * Configuration	2.342	2	1.171	7.57	<0.001***
Coding *					
Configuration					
Pulse Shape * Polarity * Configuration	5.178	2	2.589	16.73	<0.001***
Configuration					
Intensity Coding * Polarity * Configuration	0.017	1	0.017	0.11	0.738
Pulse Shape * Intensity Coding * Polarity * Configuration	0.357	2	0.179	1.15	0.315
Error	341.816	2209	0.155		
Total	421.755	2232			

Table 9

N-way ANOVA results for the vector strength ratio Channel Interaction measurements of the multipolarity experiment.

Factor	SSQ	dF	Mean SQ	F	p
Stimulus Type	0.103	2	0.051	2.42	0.09
Configuration	12.705	2	6.353	298.91	<0.001***
Stimulus Type * Configuration	0.191	4	0.048	2.25	0.06
Error	5.483	258	0.022		
Total	18.503	266			

(Macherey et al., 2006), and a stronger response of the auditory nerve has been reported using a complex masking paradigm for anodic stimulation (Macherey et al., 2008; Undurraga et al., 2010). In the present study, we did not see a systematic difference in thresholds for cathodic vs. anodic pulses, but we observed a reduced spread of excitation in monophasic and reduced channel interactions in monophasic and pseudomonophasic cathodic stimulation compared to anodic stimulation. Damage to primary afferents and somata of spiral ganglion cells generally favors anodic stimulation (Konerding et al., 2022), however, guinea pigs in this study had intact spiral ganglion cells. Thus, higher amplitude responses and lower comfortable levels with anodic stimulation may be related to more current spread with anodic stimulation and more damage to the nerve in human subjects.

The present experiments document that monophasic and pseudomonophasic stimulation patterns cause slightly less channel interaction than biphasic stimulation. This can be explained by “offsite stimulation” in monophasic pulses – anodic stimuli are more likely to activate cell bodies, while cathodic stimulation preferentially activates neurites (Ranck, 1975; Rattay, 1986). Combining the anodic and cathodic phase in biphasic stimulation thus overlaps these patterns and provides more interference if multiple active channels are used for stimulation. Accordingly, the best channel separation was achieved with monophasic

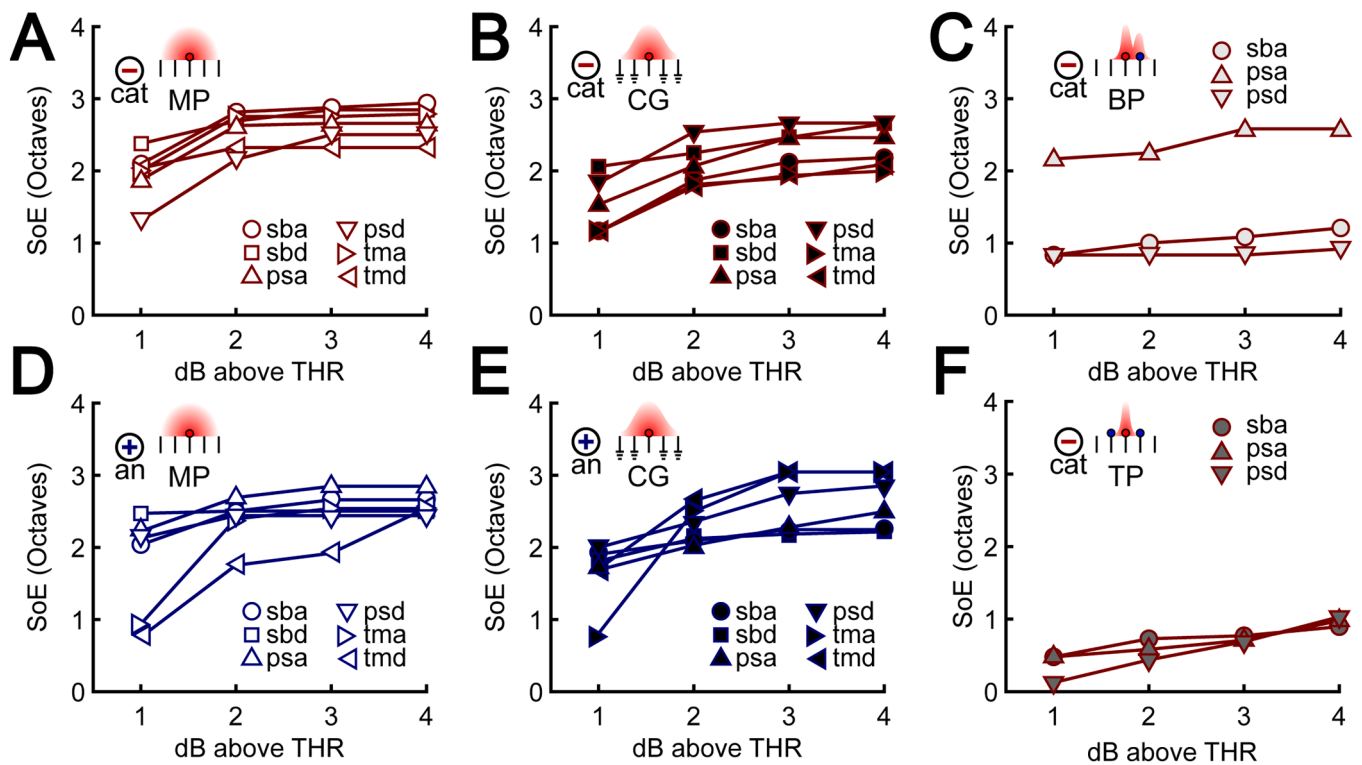


Fig. 7. The spread of excitation depends on the stimulation level. A – Spread of excitation (SoE) measured in octaves, plotted against stimulus intensity in dB above threshold for cathodic leading, monopolar stimulation (CAT-MP). Different pulse shapes are indicated with different symbols; abbreviations are the same as in Fig. 1. B – The same as A, but for common ground stimulation (CAT-CG). C – The same as A, but for bipolar stimulation (CAT-BP). D – The same as A, but for anodic leading stimulation (AN-MP). E – The same as D, but for common ground stimulation (AN-CG). F – The same as A, but for tripolar stimulation (CAT-TP).

stimulation, providing even better outcomes than pseudomonophasic stimulation.

In the light of these findings, it is not surprising that there was a significant polarity effect with monophasic stimulation. Using monophasic cathodic stimulation, channel separation was better than with anodic stimulation. This is likely due to different sites of stimulation: Microlesions in the cochlea were consistent with cathodic stimulation activating the primary afferents and anodic stimulation the axon close to soma (Konerding et al., 2022). Consequently, previous studies documented an 80-100 μ s shorter latency in anodic-leading compared to cathodic-leading stimulation (Shepherd & Javel, 1999; Miller et al., 1998). This explains why channel separation is better with cathodic stimulation: cathodic pulses activate the neurons at the primary afferents, where they have a more spread-out anatomy. With anodic stimulation affecting cells near the soma, it is more difficult to target individual axons within the bundle than with primary afferents. A spiral ganglion microlesion experiment as performed by Konerding et al. (2022) but employing true monophasic pulse shapes in combination with compound action potential measurements, would be able to test this hypothesis.

4.4. Safety considerations

We have recorded multiple benefits of monophasic or pseudomonophasic stimulation compared to biphasic stimulation, including lower thresholds, lower spread of excitation, and lower channel interactions. However, electric stimulation is only safe when charge balance is guaranteed (the used current sources included a capacitor that secured charge balance). This necessity puts into question whether this benefit of true monophasic stimulation can be translated clinically in some CI processor designs beyond the use of pseudomonophasic or passive discharge stimulation. Pseudomonophasic stimulation (with duration coding) as employed here delivers pulses with pulse durations from 150

μ s to 600 μ s, limiting these specific pulses to stimulation rates below 1666 pulses per second without factoring in the interpulse interval. To safely present even pseudomonophasic pulses consistently, an adaptive low-rate strategy thus seems necessary.

4.5. Methodological limitations

Despite the strength of combining several different stimulus parameters in one experiment, an important limitation of the present study was the use of electrode 2 for stimulation: we did not reverse the role of apical and basal electrodes in the channel interaction experiments due to the time restriction of the extensive preparation and stimuli tested. Since the base of the cochlea has larger volume than the apex (Wysocki, 2001; Liu et al., 2007; Avcı et al., 2014), the distance of the stimulating electrode to the modiolus will be different in apical vs. basal electrodes, and this may be a confounding factor (Hatsushika et al., 1990), particularly in the focused stimulation configurations. For the same reason, we could not reverse the stimulation rates at the basal and apical electrodes, and thus cannot make claims about place-dependent phase-locking differences. All this remains a topic of future study.

Due to the lengthy nature of the preparation and measurement protocol of the present experiments, we had to divide the parameter space in two and were thus not able to measure all parameter permutations in all animals. Specifically, single pulse measurements of different polarity for bipolar and tripolar stimulation could not be performed. It would be interesting to address some possible interaction effects of pulse shape, polarity, and electrode configuration in future studies, given the previously described differences in stimulus polarity effects.

Finally, our channel interaction measure is based on slow rate stimulation (19 Hz and 37 Hz). This lower limit is set by the phase locking properties of the readout structure, in our case the inferior colliculus (Liu et al., 2006). While this is far from clinical stimulation rates,

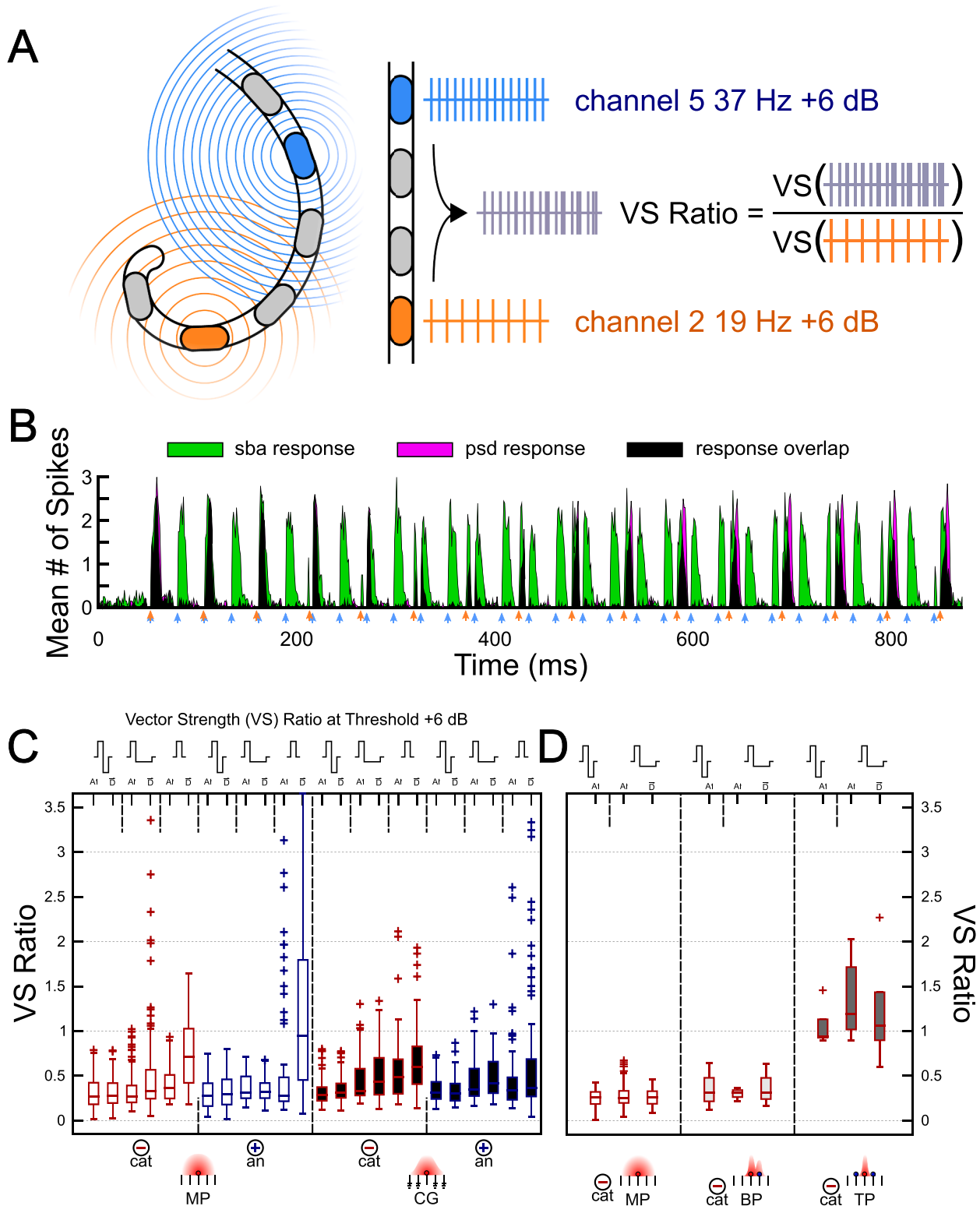


Fig. 8. Results of the channel interactions measurement. A – The channel interaction was measured by presenting a 37 Hz pulse train on electrode 5 (blue stimulus), and a 19 Hz pulse train on electrode 2 (orange stimulus), and relating the vector strength of the IC response measured at 19 Hz in response to both pulses simultaneously to the vector strength at 19 Hz to the 19 Hz train alone (“VS Ratio”). B – Example PSTHs in response to a simultaneous 19 Hz (orange arrows) and 37 Hz (blue arrows) presentation for sba (green) and psd (magenta), with the overlap depicted in black. In this example, sba pulses activate the neurons at both electrodes (responses are measured at both 19 and 37 Hz), while psd pulses activate the neurons only at electrode 2 (responses only occur at 19 Hz). C – Vector strength ratio for any given combination of stimulus properties in the common ground experiment. Plot legend and layout is the same as in Figs. 4–6. Corresponding statistics in Table 8. D – The same as in C, but for the multipolarity experiment. Corresponding statistics in Table 9. VS = vector strength.

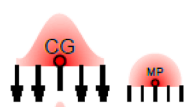
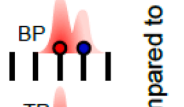

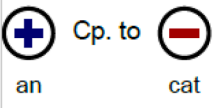
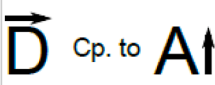
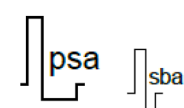
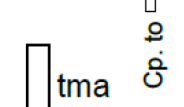
	Threshold	Dynamic Range	Spread of Excitation	Channel Interaction
	Higher (worse)	Same	Same	Same
	Higher (worse)	Higher (better)	Lower (better)	Lower (better)
	Higher (worse)	Higher (better)	Lower (better)	Lower (better)
	Same	Same	Lower for MP (better)	Same
	Same	Higher (better)	Same	Lower (better)
	Lower (better)	Same	Same	Lower (better)
	Lower (better)	Same	Lower (better)	Lower (better)

Fig. 9. Summary of the results of varying stimulation parameters as compared to their clinically most used type. Cp. to = compared to; CG = common ground; MP = monopolar; BP = bipolar; TP = tripolar; an = anodic leading (or anodic pseudomonophasic, anodic monophasic) stimulation; cat = cathodic leading (or anodic pseudomonophasic, anodic monophasic) stimulation; D = duration coding; A = current amplitude coding; psa = pseudomonophasic amplitude coding; tma = true monophasic amplitude coding; sba = standard biphasic amplitude coding.

we are confident that this measure reflects channel interactions well. Since the VS ratio is measured at 6 dB above threshold, which evokes both full overlap of electric fields as well as saturated firing rates, channel separation is likely not based purely on the temporal frequency-following properties of auditory nerve fibers. Instead, it is influenced by different firing onset and refraction times, and there are central, inhibitory, contrast-enhancing processes involved in spectral separation as well.

4.6. New signal processing strategies

The present study delineates that there is a combination of factors that contribute to improved channel separation. The standard approach of using tripolar stimulation has been very effective in the experiments at hand. Furthermore, monophasic and pseudomonophasic stimulation reduced thresholds and channel interaction, particularly in cathodic stimulation.

The results at hand suggest that there is need for new stimulation strategies in cochlear implants. These should include varying and dynamic amounts of focusing, depending on the overall loudness and spectrum of the auditory input. In faint acoustic stimuli, monopolar stimulation is more effective, conveying the temporal information robustly. As the stimulus loudness increases, the advantage is traded with the current spread that causes interference between channels in spectrally complex inputs. Here, increasing the amount of focusing by adding lateral channels of opposing polarity as in tripolar or phased-array stimulation would provide a substantial advantage. Such configurations could involve excess current that is routed to the extracochlear

electrode, as suggested previously (Kral et al., 1998; Bierer et al., 2010). However, this approach likely would not be effective in cases with varying degree of neuronal survival along the cochlear partition. Thus, the strategy would remain an option for a subpopulation of subjects with excellent cochlear health. With increasing amount of spiral ganglion survival variations, less focusing would be needed. Assuming that shorter durations of hearing loss are generally associated with better neural health (Bernhard et al., 2021), this hypothesis would predict that a rigid focusing strategy might be most effective in individuals with short durations of hearing loss. There is only limited data on this aspect. Arenberg et al. (2018) investigated the relationship of duration of deafness and vowel identification benefit of dynamic current focusing in a small data set, and found only a trend towards larger improvements in speech perception due to current focusing with shorter duration of deafness. However, duration of deafness is only a proximate for neural degeneration. Thus, ultimately a combination strategy is required that integrates the measures to determine the varying degeneration of the spiral ganglion – as already clinically applied (Bierer, 2007; Bierer et al., 2010; Arenberg Bierer, 2010; Jahn & Arenberg, 2019) – with a dynamic adjustment of the amount of current focusing used in the given subject. A biomarker of neuronal survival is thus urgently needed (Ramekers et al., 2014; Schwartz-Leyzac et al., 2023). Furthermore, pseudomonophasic stimulation strategies might further reduce channel interactions, albeit with the disadvantage of requiring hardware changes in the stimulation devices for such more complex stimulation approaches. If alternative pulse shapes can indeed reduce channel interactions without multipolar current focusing, as is indicated in the present data, this represents an alternative route to increasing spectral resolution for

individuals with poorer neural health that can be harvested clinically.

5. Conclusions

The present data using two experimental paradigms present an analysis of threshold, dynamic range, spread of excitation and channel interaction in their interdependence. The effect of common ground configuration was not significantly beneficial for reducing spread of excitation or channel interactions. The most powerful instrument in affecting spread of excitation and channel interaction was tripolar configuration. Coding of stimulus intensity by pulse duration further mildly reduced channel interactions in the time domain. Finally, monophasic and pseudomonophasic pulses also contributed to reduced channel interaction, with particular advantage when the cathodic phase was used. These results provide a solid foundation for further exploration of the stimulation parameter space of cochlear implants in the future.

CRedit authorship contribution statement

Gunnar L. Quass: Conceptualization, Funding acquisition, Data curation, Formal analysis, Investigation, Methodology, Software, Visualization, Writing – original draft, Writing – review & editing. **Andrej Kral:** Conceptualization, Funding acquisition, Methodology, Writing – original draft, Writing – review & editing.

Declaration of competing interest

Research CIs were supplied by Oticon medical. Authors have nothing to declare.

Data availability

Data will be made available on request.

Acknowledgement

The present study was supported by the William Demant Foundation and Deutsche Forschungsgemeinschaft (Exc 2177). The authors wish to thank Karl-Jürgen Kühne and Daniela Kühne for their technical assistance, and the anonymous reviewers for their helpful comments that increased the clarity of this report.

References

- Arenberg Bierer, J., 2010. Probing the electrode-neuron interface with focused cochlear implant stimulation. *Trends Amplif.* 14 (2), 84–95. <https://doi.org/10.1177/1084713810375249>.
- Arenberg, J.G., Parkinson, W.S., Litvak, L., Chen, C., Kreft, H.A., Oxenham, A.J., 2018. A dynamically focusing cochlear implant strategy can improve vowel identification in noise. *Ear Hear.* 39 (6), 1136–1145. <https://doi.org/10.1097/AUD.0000000000000566>.
- Avci, E., Nauwelaers, T., Lenarz, T., Hamacher, V., Kral, A., 2014. Variations in microanatomy of the human cochlea. *J. Comp. Neurol.* 522, 3245–3261. <https://doi.org/10.1002/cne.23594>.
- Başkent, D., 2006. Speech recognition in normal hearing and sensorineural hearing loss as a function of the number of spectral channels. *J. Acoust. Soc. Am.* 120 (5), 2908–2925.
- Battmer, R.D., Zilberman, Y., Haake, P., Lenarz, T., 1999. Simultaneous analog stimulation (SAS)-continuous interleaved sampler (CIS) pilot comparison study in Europe. *Ann. Otol. Rhinol. Laryngol. Suppl.* 177, 69–73.
- Berens, P., 2009. CircStat: A MATLAB Toolbox for Circular Statistics. *J. Stat. Softw.* 31, 293–295. <https://doi.org/10.18637/jss.v031.i10>.
- Berenstein, C.K., Mens, L.H.M., Mulder, J.J.S., Vanpoucke, F.J., 2008. Current steering and current focusing in cochlear implants: comparison of monopolar, tripolar, and virtual channel electrode configurations. *Ear Hear.* 29 (2), 250–260. <https://doi.org/10.1097/aud.0b013e3181645336>.
- Berg, K.A., Noble, J.H., Dawant, B.M., Dwyer, R.T., Labadie, R.F., Gifford, R.H., 2022. Speech recognition as a function of the number of channels for Mid-Scala electrode array recipients. *J. Acoust. Soc. Am.* 152 (1), 67. <https://doi.org/10.1121/10.0012163>.

- Bernhard, N., Gauger, U., Romo, E., Uecker, F.C., Olze, H., Knopke, S., Hänsel, T., 2021. Duration of deafness impacts auditory performance after cochlear implantation: a meta-analysis 291–301. [10.1002/hio2.528](https://doi.org/10.1002/hio2.528).
- Bierer, J.A., 2007. Threshold and channel interaction in cochlear implant users: evaluation of the tripolar electrode configuration. *J. Acoust. Soc. Am.* 121 (3), 1642–1653. <https://doi.org/10.1121/1.2436712>.
- Bierer, J.A., Bierer, S.M., Middlebrooks, J.C., 2010. Partial tripolar cochlear implant stimulation: spread of excitation and forward masking in the inferior colliculus. *Hear. Res.* 270 (1–2), 134–142. <https://doi.org/10.1016/j.heares.2010.08.006>.
- Bierer, J.A., Middlebrooks, J.C., 2004. Cortical responses to cochlear implant stimulation: channel interactions. *J. Assoc. Res. Otolaryngol.* 5 (1), 32–48. <https://doi.org/10.1007/s10162-003-3057-7>.
- Bonham, B.H., Litvak, L.M., 2008. Current focusing and steering: modeling, physiology, and psychophysics. *Hear. Res.* 242 (1–2), 141–153. <https://doi.org/10.1016/j.heares.2008.03.006>.
- Busby, P.A., Whitford, L.A., Blamey, P.J., Richardson, L.M., Clark, G.M., 1994. Pitch perception for different modes of stimulation using the cochlear multiple-electrode prosthesis. *J. Acoust. Soc. Am.* 95 (5 Pt 1), 2658–2669.
- Chatterjee, M., Fu, Q.J., Shannon, R.V., 2000. Effects of phase duration and electrode separation on loudness growth in cochlear implant listeners. *J. Acoust. Soc. Am.* 107 (3), 1637–1644.
- De Jong, M.A.M., Briaire, J.J., van der Woude, S.F.S., Frijns, J.H.M., 2019. Dynamic current focusing for loudness encoding in cochlear implants: a take-home trial. *Int. J. Audiol.* 58 (9), 553–564. <https://doi.org/10.1080/14992027.2019.1601270>.
- De Jong, M.A.M., Briaire, J.J., van der Woude, S.F.S., Frijns, J.H.M., 2019. Dynamic current focusing: a novel approach to loudness coding in cochlear implants. *Ear Hear.* 40 (1), 34–44. <https://doi.org/10.1097/AUD.0000000000000593>, 2019.
- Fishman, K.E., Shannon, R.V., Slattery, W.H., 1997. Speech recognition as a function of the number of electrodes used in the SPEAK cochlear implant speech processor. *J. Speech. Lang. Hear. Res.* 40 (5), 1201–1215.
- Friesen, L.M., Shannon, R.V., Baskent, D., Wang, X., 2001. Speech recognition in noise as a function of the number of spectral channels: Comparison of acoustic hearing and cochlear implants. *J. Acoust. Soc. Am.* 110 (2), 1150–1163. <https://doi.org/10.1121/1.1381538>.
- Gärtner, L., Lenarz, T., Ivanauskaite, J., Büchner, A., 2022. Facial nerve stimulation in cochlear implant users—a matter of stimulus parameters. *Cochlear. Implants Int.* 23 (3), 165–172.
- George, S.S., Shivdasani, M.N., Wise, A.K., Shepherd, R.K., Fallon, J.B., 2015a. Electrophysiological channel interactions using focused multipolar stimulation for cochlear implants. *J. Neural Eng.* 12 (6), 066005 <https://doi.org/10.1088/1741-2560/12/6/066005>.
- George, S.S., Wise, A.K., Fallon, J.B., Shepherd, R.K., 2015b. Evaluation of focused multipolar stimulation for cochlear implants in long-term deafened cats. *J. Neural Eng.* 12 (3), 036003 <https://doi.org/10.1088/1741-2560/12/3/036003>.
- Goldberg, J.M., Brown, P.B., 1969. Dichotic tonal stimuli: some physiological mechanisms of sound localization. *J. Neurophysiol.* 32, 613–636. <https://doi.org/10.1152/jn.1969.32.4.613>.
- Hartmann, R., Topp, G., Klinke, R., 1984. Discharge patterns of cat primary auditory fibers with electrical stimulation of the cochlea. *Hear. Res.* 13 (1), 47–62.
- Hatsushika, S., Shepherd, R.K., Tong, Y.C., Clark, G.M., Funasaka, S., 1990. Dimensions of the scala tympani in the human and cat with reference to cochlear implants. *Ann. Otol. Rhinol. Laryngol.* 99 (11), 871–876.
- Heshmat, A., Sajedi, S., Schrott-Fischer, A., Rattay, F., 2021. Polarity sensitivity from electrical stimulation of degenerated human cochlear neurons. *Front. Neurosci.* 15, 751599.
- Jahn, K.N., Arenberg, J.G., 2019. Evaluating psychophysical polarity sensitivity as an indirect estimate of neural status in cochlear implant listeners. *J. Assoc. Res. Otolaryngol.* 20 (4), 415–430. <https://doi.org/10.1007/s10162-019-00718-2>.
- Kalkman, R.K., Briaire, J.J., Dekker, D.M.T., Frijns, J.H.M., 2022. The relation between polarity sensitivity and neural degeneration in a computational model of cochlear implant stimulation. *Hear. Res.* 415, 108413.
- Konerding, W., Arenberg, J.G., Kral, A., Baumhoff, P., 2022. Late electrically-evoked compound action potentials as markers for acute micro-lesions of spiral ganglion neurons. *Hear. Res.* 413, 108057.
- Konerding, W.S., Baumhoff, P., Kral, A., 2023. Anodic polarity minimizes facial nerve stimulation as a side effect of cochlear implantation. *J. Assoc. Res. Otolaryngol.* 24 (1), 31–46.
- Kral, A., Hartmann, R., Mortazavi, D., Klinke, R., 1998. Spatial resolution of cochlear implants: the electrical field and excitation of auditory afferents. *Hear. Res.* 121 (1–2), 11–28.
- Kral, A., Tillein, J., 2021. Cochlear implants: neuroprosthetic hearing and the brain. B. *Fritsch The Senses. A Comprehensive Reference.* Academic Press, pp. 923–944.
- Kral, A., Aplin, F., Maier, H., 2021. *Prostheses for the Brain: Introduction to Neuroprosthetics.* Academic Press.
- Landsberger, D.M., Srinivasan, A.G., 2009. Virtual channel discrimination is improved by current focusing in cochlear implant recipients. *Hear. Res.* 254 (1–2), 34–41. <https://doi.org/10.1016/j.heares.2009.04.007>.
- Litvak, L.M., Spahr, A.J., Emadi, G., 2007. Loudness growth observed under partially tripolar stimulation: model and data from cochlear implant listeners. *J. Acoust. Soc. Am.* 122 (2), 967–981. <https://doi.org/10.1121/1.2749414>, 1 August.
- Liu, L.F., Palmer, A.R., Wallace, M.N., 2006. Phase-locked responses to pure tones in the inferior colliculus. *J. Neurophysiol.* 95, 1926–1935. <https://doi.org/10.1152/jn.00497.2005>.
- Liu, B., Gao, X.L., Yin, H.X., Luo, S.Q., Lu, J., 2007. A detailed 3D model of the guinea pig cochlea. *Brain Struct. Funct.* 212 (2), 223–230. <https://doi.org/10.1007/s00429-007-0146-0>.

- Loizou, P.C., 1999. Signal-processing techniques for cochlear implants. *IEEe Eng. Med. Biol. Mag.* 18 (3), 34–46.
- Macherey, O., Carlyon, R.P., van Wieringen, A., Deeks, J.M., Wouters, J., 2008. Higher sensitivity of human auditory nerve fibers to positive electrical currents. *JARO* 9 (2). <https://doi.org/10.1007/s10162-008-0112-4>.
- Macherey, O., Cazals, Y., 2016. Effects of pulse shape and polarity on sensitivity to cochlear implant stimulation: a chronic study in guinea pigs. *Adv. Exp. Med. Biol.* 894, 133–142. https://doi.org/10.1007/978-3-319-25474-6_15.
- Macherey, O., Van Wieringen, A., Carlyon, R.P., Deeks, J.M., Wouters, J., 2006. Asymmetric pulses in cochlear implants: effects of pulse shape, polarity, and rate. *J. Assoc. Res. Otolaryngol.* 7, 253–266.
- Mens, L.H.M., Berenstein, C.K., 2005. Speech perception with mono- and quadrupolar electrode configurations: a crossover study. *Otol. Neurotol.* 26 (5), 957–964. <https://doi.org/10.1097/01.mao.0000185060.74339.9d>.
- Miller, C.A., Abbas, P.J., Robinson, B.K., Rubinstein, J.T., Matsuoka, A.J., 1999. Electrically evoked single-fiber action potentials from cat: responses to monopolar, monophasic stimulation. *Hear. Res.* 130 (1-2), 197–218.
- Miller, C.A., Abbas, P.J., Rubinstein, J.T., Robinson, B.K., Matsuoka, A.J., Woodworth, G., 1998. Electrically evoked compound action potentials of guinea pig and cat: responses to monopolar, monophasic stimulation. *Hear. Res.* 119 (1-2), 142–154.
- Moon, A.K., Zwolan, T.A., Pflingst, B.E., 1993. Effects of phase duration on detection of electrical stimulation of the human cochlea. *Hear. Res.* 67 (1-2), 166–178.
- Nadol, J.B., 1990. Degeneration of cochlear neurons as seen in the spiral ganglion of man. *Hear. Res.* 49 (1-3), 141–154.
- Navtsoft, C.A., Marozeau, J., Barkat, T.R., 2020. Ramped pulse shapes are more efficient for cochlear implant stimulation in an animal model. *Sci. Rep.* 10 (1), 1–17. <https://doi.org/10.1038/s41598-020-60181-5>.
- Parkins, C.W., Colombo, J., 1987. Auditory-nerve single-neuron thresholds to electrical stimulation from scala tympani electrodes. *Hear. Res.* 31 (3), 267–285.
- Pflingst, B.E., DeHaan, D.R., Holloway, L.A., 1991. Stimulus features affecting psychophysical detection thresholds for electrical stimulation of the cochlea. I: Phase duration and stimulus duration. *J. Acoust. Soc. Am.* 90 (4 Pt 1), 1857–1866.
- Pflingst, B.E., Zwolan, T.A., Holloway, L.A., 1997. Effects of stimulus configuration on psychophysical operating levels and on speech recognition with cochlear implants. *Hear. Res.* 112 (1-2), 247–260.
- Quiroga, R.Q., Nadasdy, Z., Ben-Shaul, Y., 2004. Unsupervised spike detection and sorting with wavelets and superparamagnetic clustering. *Neural Comput.* 16, 1661–1687.
- Quass, G.L., Baumhoff, P., Gnansia, D., Stahl, P., Kral, A., 2020. Level coding by phase duration and asymmetric pulse shape reduce channel interactions in cochlear implants. *Hear. Res.* 396, 108070 <https://doi.org/10.1016/j.heares.2020.108070>.
- Ramekers, D., Versnel, H., Strahl, S.B., Smeets, E.M., Klis, S.F.L., Grolman, W., 2014. Auditory-nerve responses to varied inter-phase gap and phase duration of the electric pulse stimulus as predictors for neuronal degeneration. *J. Assoc. Res. Otolaryngol.* 15 (2), 187–202.
- Ranck, J.B., 1975. Which elements are excited in electrical stimulation of mammalian central nervous system: a review. *Brain Res.* 98, 417–440. [https://doi.org/10.1016/0006-8993\(75\)90364-9](https://doi.org/10.1016/0006-8993(75)90364-9).
- Rattay, F., 1986. Analysis of models for external stimulation of axons. *IEEE Trans. Biomed. Eng.* 33, 974–977.
- Sato, M., Baumhoff, P., Kral, A., 2016. Cochlear implant stimulation of a hearing ear generates separate electrophonic and electroneural responses. *J. Neurosci.* 36 (1), 54–64. <https://doi.org/10.1523/JNEUROSCI.2968-15.2016>.
- Schvartz-Leyzac, K.C., Colesa, D.J., Swiderski, D.L., Raphael, Y., Pflingst, B.E., 2023. Cochlear health and cochlear-implant function. *J. Assoc. Res. Otolaryngol.* <https://doi.org/10.1007/s10162-022-00882-y>.
- Shepherd, R.K., Javel, E., 1999. Electrical stimulation of the auditory nerve: II. Effect of stimulus waveshape on single fibre response properties. *Hear. Res.* 130 (1-2), 171–188.
- Spitzer, E.R., Hughes, M.L., 2017. Effect of stimulus polarity on physiological spread of excitation in cochlear implants. *J. Am. Acad. Audiol.* 28, 786–798. <https://doi.org/10.3766/jaaa.16144>.
- Throckmorton, C.S., Collins, L.M., 2002. The effect of channel interactions on speech recognition in cochlear implant subjects: Predictions from an acoustic model. *J. Acoust. Soc. Am.* 112 (1), 285–296.
- Undurraga, J.A., Carlyon, R.P., Wouters, J., Van Wieringen, A., 2013. The polarity sensitivity of the electrically stimulated human auditory nerve measured at the level of the brainstem. *JARO - J. Assoc. Res. Otolaryngol.* 14, 359–377. <https://doi.org/10.1007/s10162-013-0377-0>.
- Undurraga, J.A., van Wieringen, A., Carlyon, R.P., Macherey, O., Wouters, J., 2010. Polarity effects on neural responses of the electrically stimulated auditory nerve at different cochlear sites. *Hear. Res.* 269 (1-2), 146–161. <https://doi.org/10.1016/j.heares.2010.06.017>.
- van den Honert, C., Kelsall, D.C., 2007. Focused intracochlear electric stimulation with phased array channels. *J. Acoust. Soc. Am.* 121 (6), 3703–3716. <https://doi.org/10.1121/1.2722047>.
- Van Wieringen, A., Carlyon, R.P., Laneau, J., Wouters, J., 2005. Effects of waveform shape on human sensitivity to electrical stimulation of the inner ear. *Hear. Res.* 200 (1-2), 73–86.
- White, M.W., Merzenich, M.M., Gardi, J.N., 1984. Multichannel cochlear implants. Channel interactions and processor design. *Arch. Otolaryngol.* 110 (8), 493–501.
- Wysocki, J., 2001. Dimensions of the vestibular and tympanic scalae of the cochlea in selected mammals. *Hear. Res.* 161 (1-2), 1–9.
- Zierhofer, C.M., Hochmair-Desoyer, L.J., Hochmair, E.S., 1995. Electronic design of a cochlear implant for multichannel high-rate pulsatile stimulation strategies. *IEEE Trans. Rehab. Eng.* 3 (1), 112–116.